Impact of Ca(II) on the aqueous speciation, redox behavior, and environmental mobility of Pu(IV) in the presence of EDTA

Nicole A. DiBlasi [a], Agost G. Tasi [b], Xavier Gaona [b,*], David Fellhauer [b], Kathy Dardenne [b], Jörg Rothe [b], Donald T. Reed [c], Amy E. Hixon [a,*], Marcus Altmaier [b]

[a] Department of Civil & Environmental Engineering & Earth Sciences, University of Notre Dame, 301 Stinson-Remick, Notre Dame, IN 46556, United States of America
[b] Karlsruhe Institute of Technology, Institute for Nuclear Waste Disposal, P.O. Box 3640, 76021 Karlsruhe, Germany
[c] Los Alamos National Laboratory, 1400 University Dr., Carlsbad, NM 88220, United States of America

HIGHLIGHTS

- Previous models overestimate Pu solubility with EDTA under alkaline conditions.
- Reevaluation of log $\beta^{\circ}_{(1,x,1)}$ based on new experimental data and published results
- Newly defined model accurately describes trends across a wide range of parameters.
- Evidence for the formation of a quaternary Ca Pu(IV) OH EDTA complex was found.
- Pu interactions with organic ligands and other di/trivalent cations can be relevant.

GRAPHICAL ABSTRACT

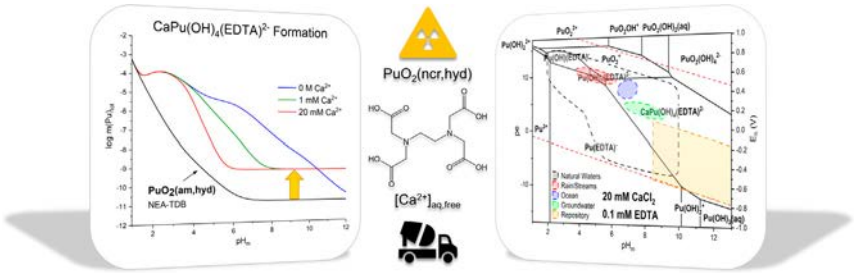

ARTICLE INFO

Keywords:
Plutonium
EDTA
Calcium
Complexation
Thermodynamics
XANES
EXAFS

ABSTRACT

The impact of calcium on the solubility and redox behavior of the Pu(IV) EDTA system was investigated using a combination of undersaturation solubility studies and advanced spectroscopic techniques. Batch solubility experiments were conducted in 0.1 M NaCl NaOH HCl EDTA $CaCl_2$ solutions at constant [EDTA] = $1{\cdot}10^{-3}$ M, $1 \le pH_m \le 11$, and $1{\cdot}10^{-3}$ M $\le [CaCl_2] \le 2{\cdot}10^{-2}$ M. Additional samples targeted brine systems represented by 3.5 M $CaCl_2$ and WIPP simulated brine. Redox conditions were buffered with hydroquinone (pe + pH ≈ 9.5) with selected samples prepared in the absence of any redox buffer. All experiments were performed at T = 22 °C under Ar atmosphere. In situ X ray absorption spectroscopy indicated that PuO_2(ncr,hyd) was the solubility controlling phase during the lifetime of all experiments and that aqueous plutonium was present in the +IV oxidation state across all experimental conditions except at $pH_m \approx 1$, where a small fraction of Pu(III) was also identified. Current thermodynamic models overestimate Pu(IV) EDTA solubility in the absence of calcium by approximately 1 1.5 $\log_{10}$ units and do not describe the nearly pH independent, increased solubility observed with increased calcium concentrations. The ternary Pu(IV) OH EDTA system without calcium was reevaluated using solubility data obtained in this work and reported in the literature. An updated thermodynamic model including the complexes $Pu(OH)(EDTA)^-$, $Pu(OH)_2(EDTA)^{2-}$, and $Pu(OH)_3(EDTA)^{3-}$ was derived. Solubility data collected in the presence of calcium follows a pH independent trend ($\log m(Pu)_{tot}$ vs. pH_m), which can only be explained by assuming the formation of a quaternary complex, tentatively defined as $CaPu(OH)_4(EDTA)^{2-}$, in solution. The significant enhancement of plutonium solubility observed in the investigated brine systems supports the formation of a quaternary complex that is not outcompeted by $Ca(EDTA)^{2-}$, even in concentrated $CaCl_2$ solutions. Although the

* Corresponding authors.
E-mail addresses: xavier.gaona@kit.edu (X. Gaona), ahixon@nd.edu (A.E. Hixon).

exact stoichiometry of the complex may need to be revisited, this new quaternary complex has a pronounced im pact on plutonium predominance diagrams over a broad range of pH, pe, and calcium concentrations that are rel evant to nuclear waste disposal.

1. Introduction

The consensus among the international community is that the most favored means of disposal for high level and long lived radioactive wastes is in a deep geologic repository (Geckeis et al., 2019; IAEA, 2003). To support international waste disposal efforts, interactions and processes that could potentially lead to the release of radionuclides into the geosphere in case of water intrusion or damage to the integrity of such a facility must be well understood. Of these radionuclides, pluto nium is important due to its prevalence in both commercial waste and defense related transuranic waste, high alpha radiotoxicity, and long half life ($t_{1/2}$ $^{239}Pu = 2.41{\cdot}10^4$ a), which allows it to persist and contribute to the overall activity of the waste for over one hundred thousand years.

The design of deep geologic repositories involves a combination of both natural and engineered barriers that define the geochemical boundary conditions within the repository. After repository closure, strongly reducing conditions are expected to develop due to the anoxic corrosion of iron and steel present in the repository. The use of cemen titious materials is considered in repository concepts for the stabiliza tion of the waste and for construction purposes. Upon interaction with groundwater, the progressive degradation of cement or the presence of other engineered barrier materials, such as MgO, will buffer the pH in the hyperalkaline to alkaline range, respectively, strongly affecting the chemical behavior of the radionuclides.

Ethylenediaminetetraacetic acid (EDTA) has been used extensively in the nuclear industry through the processing of plutonium containing wastes, in the defense production of plutonium, and as a decontamina tion agent (Ayres, 1970; McFadden, 1980; Rai et al., 2008). It has been co disposed with plutonium in many waste streams, some of which were inadvertently released into the environment (Freeman Pollard et al., 1994; Rai et al., 2008). EDTA is a strong chelating ligand that forms a wide range of stable aqueous complexes with plutonium in the +III, +IV, and +V oxidation states (AlMahamid et al., 1996; Boukhalfa et al., 2004; DiBlasi et al., 2021; Hummel et al., 2005; Reed et al., 1998) and several other metal cations. Depending upon the boundary conditions, plutonium EDTA complexation may enhance the solubility of plutonium and decrease its retention, thus having a notable impact on the environmental mobility of this radionuclide (Boukhalfa et al., 2004; Meyer et al., 2007; Rai et al., 2008).

Plutonium has four relevant oxidation states in aqueous systems: +III, +IV, +V, and +VI. Each oxidation state has its own characteristic environmental chemistry and mobility. Because the reduction poten tials of plutonium are similar between vicinal states under pertinent boundary conditions, preferential complexation can have a significant influence on the final oxidation state distribution of plutonium in the presence of a ligand. Reed et al. (1998) observed the reduction of Pu (VI) to Pu(V) and Pu(IV) in the presence of three organic complexants that are expected to be present in geologic repositories: EDTA ($C_{10}H_{16}N_2O_8$), citrate ($C_6H_8O_7$), and oxalate ($C_2H_2O_4$). While the reduc tion kinetics vary for each organic molecule, the authors reported the stabilization of plutonium in its +IV oxidation state in the presence of each of the three ligands. Additionally, a recent paper by DiBlasi et al. (2021) presented evidence on increasing Pu(IV) fraction over time orig inating from both Pu(V/VI) or Pu(III) aqueous species under alkaline conditions in the presence of EDTA and absence of any redox buffer. Thus, organic complexation may contribute to plutonium oxidation state distribution, which is constantly evolving in complex matrices with other redox active elements, such as iron, present.

Calcium is expected in geological repositories due to its ubiquity in environmental systems and host rock formations. Cementitious mate rials are also a prevalent source of calcium in some repository concepts, often in the form of calcium silicate hydrate (C S H) phases and portlandite ($Ca(OH)_2$) (Berner, 1992; Lucchini et al., 2013; Wieland and Van Loon, 2003). In brine systems, the corrosion of cementitious waste forms in the presence of concentrated $MgCl_2$ solutions can also result in $CaCl_2$ rich brines (up to 4 M) with high pH values ($pH_m \approx$ 12) in cases where specific stoichiometric requirements are fulfilled (Bube et al., 2013). Calcium forms a prominently stable complex with EDTA ($\log \beta^\circ(Ca(EDTA)^{2-}) = (12.69 \pm 0.06)$), which can decrease the free ligand concentration available for complexation with radionu clides over a broad pH range (~ 3 14) (Hummel et al., 2005). However, calcium can also act as a stabilizing counter ion for negatively charged complexes, thus promoting the formation of stable ternary/quaternary complexes Ca RN L or Ca RN OH L (RN = radionuclide). Such com plexes have been described for lanthanides and actinides with other chelating ligands like gluconate (GLU, $C_6H_{12}O_7$), isosaccharinic acid (ISA, $C_6H_{12}O_6$), and citrate (Felipe Sotelo et al., 2015; Rojo et al., 2021; Tasi et al., 2018a, 2018b; Tits et al., 2005; Vercammen et al., 2001).

Currently, the only operational deep geologic repository in the United States of America is the Waste Isolation Pilot Plant (WIPP) in Carlsbad, New Mexico. The WIPP is located 655 m (2,150 ft) under ground in the Salado Formation and is designed to accept defense trans uranic (TRU) waste. As of 2019, the WIPP inventory accounts for the co disposal of approximately $4.03{\cdot}10^2$ kg EDTA (up to ~$8{\cdot}10^{-5}$ M) and $1.56{\cdot}10^4$ kg plutonium (but an additional 32 metric tons is under con sideration). The approximate molar concentration of EDTA was calcu lated by dividing the total moles in the WIPP inventory by the minimum brine volume (17,400 m^3), as reported in the 2019 Compli ance Recertification Application for the Waste Isolation Pilot Plant (Appendix SOTERM 2019, 2019). The addition of MgO as a buffer pro motes alkaline conditions with the expected pH_m of ~9 ($pH_m = -\log [H^+]$, with $[H^+]$ in molal units), and both anoxic and strongly reducing conditions are expected post closure (Appendix SOTERM 2019, 2019). Although NaCl and $MgCl_2$ are expected to be the main brine compo nents upon the occurrence of a water intrusion scenario at the WIPP, in digenous calcium concentrations in the brine are estimated to be 7 20 mM (Appendix SOTERM 2019, 2019; Lucchini et al., 2013) and could be higher if the anhydrite present in the Salado Formation interbeds is considered.

In this work, we investigated the solubility, complexation, and redox behavior of plutonium in the presence of EDTA and calcium. Experi ments were performed under controlled redox conditions using a com bination of solubility experiments and advanced spectroscopic techniques. Special focus was given to the specific role of calcium in this system, which can act either as a competitor with plutonium for EDTA complexation, or as a component contributing to the formation of stable quaternary Ca Pu OH EDTA complexes not described before. On the basis of our own experimental data and previous solubility stud ies, this work aims to construct a comprehensive thermodynamic de scription of this system under conditions relevant for nuclear waste disposal.

2. Thermodynamic background

The speciation of plutonium in the presence of ethylenediaminetet raacetic acid (EDTA) has been investigated in numerous studies by

means of ion exchange, solvent extraction, solubility, spectrophotometry, electromigration, polarography, cyclic voltammetry, and potentiometric titration since the late 1950s (AlMahamid et al., 1996; Boukhalfa et al., 2004; Cauchetier and Guichard, 1975, 1973; Foreman and Smith, 1957a, 1957b; Gel'man et al., 1959; Merciny et al., 1978; Meyer et al., 2007; Mikhailov, 1969; Moskvin and Artyukhin, 1959; Poczynajł-o, 1989, 1991; Rai et al., 2001, 2008, 2010; Reed et al., 1998; Stepanov and Makarova, 1965; Thakur et al., 2009). The most comprehensive critical review of thermodynamic studies dedicated to the interaction of radionuclides with selected organic ligands of relevance for nuclear waste disposal (oxalate, citrate, EDTA, and isosaccharinic acid) was published in 2005 within the Thermochemical Database project of the Nuclear Energy Agency (NEA TDB) (Hummel et al., 2005). Thermodynamic data selected for the Pu EDTA system within the NEA TDB is the basis of the thermodynamic calculations performed in this work. Only Pu(III) EDTA complexes are currently selected in the NEA TDB, with $\log \beta^{\circ}(\mathrm{Pu(EDTA)^-}) = (20.180 \pm 0.370)$ and $\log \beta^{\circ}(\mathrm{Pu(HEDTA)(aq)}) = (22.020 \pm 0.260)$. Thermodynamic studies available on the Pu(IV) EDTA system were not considered reliable by the NEA reviewers, who recommended the use of data selected for U(IV) and Np(IV) for scoping calculations with Pu(IV).

Three major Pu(IV) EDTA thermodynamic studies were published after the most recent NEA TDB review, and thus were not included in the thermodynamic data selection process (Boukhalfa et al., 2004; Meyer et al., 2007; Rai et al., 2008). Boukhalfa et al. (2004) utilized a combination of techniques, including spectrophotometry under acidic conditions with $I = 1.0$ M, potentiometric titration from pH 0–10 with $I = 0.1$ M, and cyclic voltammetry at pH ≤ 8.2 with $I = 0.1$ M, to develop their speciation model. All experiments were performed using sodium salts as the ionic media (i.e., $NaCl/HClO_4$, $NaNO_3$, or NaCl). The model consists of six Pu(IV) EDTA species: Pu(EDTA)(aq), $\mathrm{Pu(OH)(EDTA)^-}$, $\mathrm{Pu(OH)_2(EDTA)^{2-}}$, $\mathrm{Pu(EDTA)_2^{4-}}$, $\mathrm{Pu(EDTA)_2H^{3-}}$, and $\mathrm{Pu(EDTA)_2H_3^-}$. Plutonium (~93% ^{239}Pu) concentrations ranged from $2.49{\cdot}10^{-5}$ M for potentiometric titrations to $1.9{\cdot}10^{-3}$ M for spectrophotometry, and as high as $5{\cdot}10^{-3}$ M for cyclic voltammetry. Due to these relatively high concentrations, precipitation was observed for titrations above pH 7.5, limiting the data analysis to lower pH. Additionally, calculations by Boukhalfa et al. (2004) involved the use of formation constants at various ionic strengths without the implementation of ionic strength corrections. This oversight was later corrected by Rai et al. (2008) in their detailed analysis of these data.

Meyer et al. (2007) also utilized potentiometric titrations from pH 1.6–10 at $I = 1.0$ M and spectrophotometric titrations at pH 1.6 with constant $I = 1.0$ M using KNO_3 as the ionic medium to develop their Pu(IV) EDTA speciation model. This model consists of five Pu(IV) EDTA species: Pu(EDTA)(aq), $\mathrm{Pu(OH)(EDTA)^-}$ $\mathrm{Pu(EDTA)_2^{4-}}$, $\mathrm{Pu(EDTA)_2H^{3-}}$ and $\mathrm{Pu(EDTA)_2H_2^{2-}}$. Unlike Boukhalfa et al. (2004), Meyer et al. (2007) implemented SIT ionic strength corrections to extrapolate equilibrium constants to zero ionic strength, and additional complexation interactions with ionic media were considered and corrected for during data analysis. Plutonium (~98% ^{239}Pu) concentrations were kept sub millimolar with very low titration rates to minimize localized oversaturations that would lead to colloid or solid formation. Even so, precipitates were observed at pH ≥ 7. Equilibrium constants were determined using only potentiometric titration data with one or two equivalents of EDTA. Similar to Boukhalfa et al. (2004), spectrophotometry was only performed under acidic conditions and thus provided very little supporting evidence regarding Pu(IV) EDTA speciation, particularly at higher pH where the solubility models differ and precipitation may have affected the potentiometric titration data. The authors address the precipitation within their work and limit their data to pH ≤ 6.5, but still extrapolate to produce a speciation model out to pH 10 that does not agree with either of the two other Pu(IV) EDTA speciation models discussed here.

The third and final study not included in the most recent NEA TDB review is Rai et al. (2008). This paper is based on the experimental results reported in a previous publication by the same authors, Rai et al. (2001), which was also not discussed within the NEA TDB review. Rai and co-workers conducted solubility experiments from undersaturation conditions using PuO_2(am,hyd), which overcomes the problems under alkaline conditions reported by both Boukhalfa et al. (2004) and Meyer et al. (2007) that resulted in the formation of colloidal or nanocrystalline solid phases. Solubility data was collected from pH 2–11 and the aqueous plutonium oxidation state was verified using solvent extraction procedures. The authors used their solubility data points after 7–10 days of equilibration to derive thermodynamic and Pitzer activity models, which consist of three predominant Pu(IV) EDTA species: $\mathrm{Pu(OH)(EDTA)^-}$, $\mathrm{Pu(OH)_2(EDTA)^{2-}}$, and $\mathrm{Pu(OH)_3(EDTA)^{3-}}$. Rai et al. (2008) evaluated the possible formation of the unhydrolyzed Pu(EDTA)(aq) complex in their study but found that this species was not needed to effectively model their solubility data. The main differences between the 2001 and 2008 publications were the acidity constants of EDTA and the solubility product of PuO_2(am,hyd) used; in the 2008 publication the selected values were consistent with the NEA TDB (Guillaumont et al., 2003; Hummel et al., 2005). It is of note, however, that the solid phase was not characterized in the original publication by Rai et al. (2001). In addition to evaluating their own data, Rai et al. (2008) also reevaluated the data of Boukhalfa et al. (2004) to determine the importance of 1:2 Pu(IV) EDTA complexes. Upon revisiting the data of Boukhalfa et al. (2004) with appropriate ionic strength corrections and consistent equilibrium constants, Rai et al. (2008) determined that the model proposed by Boukhalfa et al. (2004) no longer fit their data. More specifically, the 1:2 Pu(IV) EDTA complexes proposed by Boukhalfa et al. (2004) were not necessary to describe their data at pH ≤ 9.

All of the models include mixed Pu(IV) OH EDTA species and, hence, depict a pH dependent trend in the solubility curve where total plutonium concentrations are expected to smoothly decrease with increasing alkalinity of the system. Even with the short equilibrium times utilized in their study (7–10 days), Rai et al. (2008) is considered the most reliable study due to the extensive variation of the applied experimental parameters and the use of an experimental approach which overcomes artifacts in alkaline conditions. For these reasons, the work of Rai et al. (2008) is taken as the basis for the discussion of the Pu(IV) EDTA system.

The NEA TDB selects two Ca EDTA species $\mathrm{Ca(EDTA)^{2-}}$ and $\mathrm{Ca(HEDTA)^-}$ and both complexes have been considered in this work for the thermodynamic calculations in the presence of calcium (Hummel et al., 2005). The possible formation of the complex $\mathrm{Ca_2(EDTA)(aq)}$ was reported in Schwarzenbach and Ackermann (1947), Anderegg et al. (1975), and Arena et al. (1983), but these references were not considered reliable by the NEA TDB. Due to the great stability of the $\mathrm{Ca(EDTA)^{2-}}$ complex, the presence of calcium has been generally assumed to outcompete the complexation of EDTA with other metal ions present in significantly lower concentrations (see for instance the discussion in Rai et al. (2008)). Additionally, calcium has been shown to form ternary Ca Pu(IV) OH complexes, as reported by Altmaier et al. (2008). The ternary complex $\mathrm{Ca_4[Pu(OH)_8]^{4+}}$ is expected form and impact plutonium solubility in concentrated calcium solutions ($[\mathrm{Ca(II)}] \geq 2.0$ M) at $\mathrm{pH_m} > 11$; to assess its role in the quaternary Ca-Pu(IV)-EDTA-H_2O system, we have included this complex in the calculations performed within this work.

The thermodynamic calculations in this work are based on the reactions and associated constants reported in the literature (Table A1) or as updated within this work (Table 2). Literature complexation constants with EDTA were selected from Rai et al. (2008) and the NEA TDB (Hummel et al., 2005). The Specific Ion interaction Theory (SIT) was used for ionic strength corrections (Ciavatta, 1980; Pitzer, 1991), and the ion interaction parameters (Table A2) were either taken from the literature (Grenthe et al., 2020; Guillaumont et al., 2003; Hummel et al., 2005; Neck et al., 2009; Neck and Kim, 2001) or estimated based on the charge correlation approach described by Hummel (2009).

3. Experimental

3.1. Materials

Experiments with plutonium were performed in specialized laboratories in the controlled area of KIT INE. All experiments were conducted in argon gloveboxes with $O_2 < 2$ ppm and under carbonate exclusion. All experimental solutions were prepared with ultra pure water purified with a Milli Q apparatus (Millipore, 18.2 MΩ, 22 ± 2 °C). Before use, Milli Q water was boiled for several hours while being purged with argon gas. EDTA stock solutions were prepared from H_4EDTA (purified grade ≥ 98.5%) and corresponding sodium salts (Sigma Aldrich) to target specific pH values: Na_2H_2EDTA (99.0 101.0%), $Na_3HEDTA{\cdot}xH_2O$ (≥95%), and $Na_4EDTA{\cdot}2H_2O$ (99.0 101.0%). Calcium containing solutions were prepared with $CaCl_2{\cdot}2H_2O$ (Merck, p.a.). Redox buffers were prepared using hydroquinone (Merck, p.a., hereafter denoted as HQ) and $Na_2S_2O_4$ (Merck, ≥ 87%). TRIS buffer solutions were prepared with predetermined ratios of Trizma® base and Trizma® hydrochloride, as purchased (Sigma Aldrich, p.a.). Ionic strength in indicated systems was kept constant at $I = 0.1$ M using NaCl (Merck, p.a.). The 0.1 M NaOH and HCl solutions used for pH adjustments were prepared from standard solutions (Merck, Titrisol®). Plutonium solids were prepared from a plutonium stock in 2.0 M $HClO_4$ with an isotopic composition of 99.4% ^{242}Pu, 0.58% ^{239}Pu, 0.005% ^{238}Pu, and 0.005% ^{241}Pu.

3.2. Preparation of plutonium solid phases

Details on the synthesis procedure and the characterization results of the nanocrystalline PuO_2(ncr,hyd) solid phase used in the current study are published elsewhere (Tasi et al., 2018c). By the initialization of these experiments, the PuO_2(ncr,hyd) phase had aged ca. 11 years in 0.10 M NaCl HCl media ($pH_c \approx 4$).

The solid phase $Pu(OH)_3$(am) was freshly synthesized and used as a reference material for X ray absorption spectroscopic (XAS) analyses. A Pu(IV) stock solution in 2 M $HClO_4$ was reduced electrochemically with a platinized Pt wire working electrode to $Pu(III)_{aq}$ by applying a potential range of −0.20 to −0.40 V (vs. SHE) with the use of an Ag/AgCl/3 M NaCl reference electrode (Metrohm) and a standard Pt electrode acting as counter electrode. The reference and counter electrodes were separated from the plutonium stock by ceramic diaphragms and Teflon capillaries filled with 1.7 M $HClO_4$ solutions attached to quartz tubes. The three electrodes were connected to a potentiostat (Princeton Applied Research Model 362) to control constant voltage. To avoid overheating, the current never exceeded 10 mA. The procedure was monitored by means of visible near infrared (Vis NIR) absorption spectroscopy on a single beam diode array photometer (λ = 400 1020 nm, Carl Zeiss AG, MSC 501). The electrochemically prepared Pu(III) stock solution was precipitated as $Pu(OH)_3$(am) by its slow addition to a TRIS buffer solution ($pH_m = 9.47$) with 5 mM $Na_2S_2O_4$ redox buffering agent present. The resulting solid phase was used as the reference material in the X ray absorption near edge structure (XANES) study.

3.3. Solubility experiments

Batch type undersaturation solubility experiments using PuO_2(ncr,hyd) were carried out at a constant total EDTA concentration of 1 mM with varying pH_m and total $CaCl_2$ concentrations. Table A3 details the experimental conditions for each individual batch experiment. The ionic strength in most systems was kept constant at 0.10 M accounting for the contribution of all the components: Na_4EDTA Na_3HEDTA Na_2H_2EDTA NaCl HCl NaOH $CaCl_2$. Exceptions were the samples with the highest calcium concentration ($[CaCl_2] = 3.5$ M, $I = 10.5$ M) and the samples prepared in the WIPP simulated brine (see Table A4 for brine formulation). The pH_m of each sample was adjusted using appropriate concentration solutions of HCl and NaOH to maintain constant ionic strength. After the specific amounts of suspended PuO_2(ncr,hyd) solid phase (in aliquots of 0.1 M NaCl solutions) were added to the samples, values of pH_m, E_h, and aqueous plutonium concentrations (after 10kD ultrafiltration) were monitored in all systems up to 73 days.

3.4. Solution characterization analytical methods

All pH measurements were performed using a combination pH electrode (type Orion Ross, Thermo Scientific™) freshly calibrated against standard pH buffers (pH = 3 13, Merck). To account for any ionic strength effects, we report pH as pH_m ($pH_m = -\log(H^+) = pH_{exp} + A_m$), or the total free concentration of protons in molal units. In aqueous solutions of ionic strength $I \geq 0.1$ M, the measured pH value (pH_{exp}) is an operational, apparent value related to (H^+) by A_m, an empirical parameter that includes the activity coefficient of the proton (γH^+) and the liquid junction potential of the electrode for a given background electrolyte, ionic strength, temperature, and pressure. Empirical A_m values for NaCl and $CaCl_2$ systems were adapted from elsewhere (Altmaier et al., 2003, 2008).

The redox potential in solution was determined with combined Pt or Au and Ag/AgCl reference electrodes (Metrohm). The measured potentials were converted to E_h through a standard correction for the potential of the Ag/AgCl inner reference electrode at 3 M KCl and T = 22 °C (+207 mV). E_h values were further converted to pe ($pe = -\log a_{e^-}$) by Eq. (1):

$$E_h \quad -RTln(10)\,F^{\ 1}\,log\,a_e \qquad RTln(10)\,F^{\ 1}\,pe \tag{1}$$

where R is the ideal gas constant (8.31446 $J\,mol^{-1}\,K^{-1}$), F is the Faraday constant (96,485.33 $C\,mol^{-1}$), and a_{e^-} is the activity of the electron. Each redox potential measurement was allowed a minimum of 15 min for equilibration until the absolute drift of the value was observed to be below 3.0 mV min^{-1}. Additional, hour long measurements were taken periodically after cleaning the electrode with 1.0 M HCl to verify the validity of the values obtained through the 15 min measurements. The latter acquisitions resulted in an absolute electrode drift of ≤0.5 mV min^{-1}. Overall uncertainties of measured E_h values (calculated as 2σ of repeated measurements) ranged between ±15 and ± 40 mV.

The total molar aqueous plutonium concentration ($(Pu)_{tot}$) was quantified after phase separation using quadrupole inductively coupled plasma mass spectrometry (ICP MS, PerkinElmer™ NexION® 2000) and/or sector field ICP MS (SF ICP MS, Thermo Scientific™ ELEMENT™). Phase separation was achieved on an aliquot of the original sample through 10 kD centrifugal filters (pore size ≈ 2 3 nm, Nanosep®, Pall Life Sciences) at 6000 rpm for 15 min. The filtrates were directly diluted in 2% HNO_3 before analysis. Molar concentrations ($mol{\cdot}L^{-1}$) were converted to molal units ($mol{\cdot}kg_w^{-1}$, $m(Pu)_{tot}$) using the conversion factors reported elsewhere (Grenthe et al., 2020).

3.5. X ray absorption spectroscopy

XANES and Extended X ray Absorption Fine Structure (EXAFS) of selected aqueous and solid phases were recorded at the INE Beamline for Actinide Research at the Karlsruhe Research Accelerator (KARA), KIT Campus North (Rothe et al., 2012, 2019). The storage ring operated at 2.5 GeV electron energy with a mean electron current of 120 mA. Solid phases were retrieved and characterized by XANES and EXAFS analyses to gain insight on the plutonium solid phase controlling the solubility in the undersaturation experiments. Aqueous phases were retrieved and characterized to experimentally determine the oxidation state distribution of plutonium in solution.

For the purpose of these analyses, selected plutonium samples were transferred into polyethylene vials under an argon atmosphere. A suspension of approximately 1 mg of the solid material was pipetted into the vial, tightly sealed with Parafilm® (Bemis Company, Inc.), and centrifuged for a minimum of 10 min at 6000 rpm to compact the solid on the bottom of the vial. Once the solid was sufficiently compacted, this

sample vial was used for both aqueous and solid phase analyses. This method allowed for the collection of XAS measurements without disturbing the system equilibrium. Following solid compaction, the vials were then mounted using Kapton® tape into a gas tight cell within an argon glovebox and transported to the INE Beamline. During measurements, argon was continuously flushed through the cell ensuring the presence of an inert atmosphere.

XAS spectra of the Pu L_{III} edge (18,057 eV) were recorded in fluorescence detection mode using a combination of two Silicon Drift Detectors (SDD) a Vortex® ME4 (4 elements) and a Vortex® 60EX (1 element) (Hitachi/SIINT, both 1 mm crystal thickness). Incident beam intensity and the transmission of a reference 20 μm zirconium metal foil were recorded simultaneously using argon filled ionization chambers at ambient pressure; 3 9 scans were collected for each sample.

For a selected number of samples, before and after the XAS measurements, oxidation states of aqueous plutonium species were further verified by Vis NIR spectrophotometry. The latter analyses were performed on ultrafiltered aliquots of the XAS aqueous sample in the range of $\lambda =$ 400 1020 nm. In all cases, these measurements indicated no beam induced effects imposed on the samples during XAS analysis.

XANES and EXAFS data reduction were performed with the ATHENA and ARTEMIS software from the Demeter 0.9.26 program package (Ravel and Newville, 2005) following standard procedures. The Pu L_{III} edge XANES spectra obtained in this work were calibrated against the first inflection point in the K edge spectrum of the zirconium metal foil (K edge = 17,998 eV) and averaged to reduce statistical noise. E_0 for the Pu L_{III} edge was selected at the white line maxima. The spectra were then compared with Pu(III), Pu(IV), $Pu(OH)_3$(am), and PuO_2(ncr, hyd) reference spectra collected at the INE Beamline under similar experimental conditions and data analysis procedures (Brendebach et al., 2009; Tasi et al., 2018c). EXAFS data analysis was based on standard least squares fit techniques. Neighbor atom distances (R_i), EXAFS Debye Waller factors (σ_i^2), and coordination numbers (N_i) for the different coordination shells (i) were determined using the FEFFIT code (FEFF6) within the Demeter 0.9.26 program package. The crystallographic information file (COD 9009036) for the fluorite structure of PuO_2 was obtained from the Crystallography Open Database and used to calculate the FEFF backscattering amplitude and phase shift functions for single scattering paths (Gražulis et al., 2012; Wyckoff, 1963). All fit operations were performed in R space over the individual radial distance ranges as described in Section 4.2. The amplitude reduction factor (S_0^2) was fixed at 1.0.

3.6. Data analysis and thermodynamic modeling

Equilibrium thermodynamic calculations were conducted using constants reported in the literature (Table A1) or updated constants from this work (Table 2). The PHREEPLOT PHREEQC Interactive software package was applied for solubility calculations and data analysis/modeling (version 3.4.0, svn 12927) (Charlton and Parkhurst, 2011; Kinniburgh and Cooper, 2011; Parkhurst and Appello, 1999, 2013). The Medusa/Spana software package was applied for calculation of Pourbaix (pe pH_m) diagrams (Puigdomenech, 2020).

4. Results and discussion

4.1. Impact of EDTA and calcium on the Pu(III)/Pu(IV) redox border measurements of (pe + pH_m) and Pourbaix diagrams

The redox borderline between Pu(III) and Pu(IV) indicating a 50% to 50% distribution of the Pu(III) and Pu(IV) oxidation states is an important indicator to assess the environmental mobility of plutonium. Fig. A1 in the Appendix shows the Pourbaix (pe pH_m) diagram of aqueous plutonium calculated in the absence of EDTA and calcium (Fig. A1a), in the presence of 1 mM EDTA (Fig. A1b), and in the presence of 1 mM EDTA and 20 mM $CaCl_2$ (Fig. A1c) (using the model published in Rai et al. (2008)). Fig. A1b shows that the addition of EDTA shifts the aqueous Pu(III)/Pu(IV) boundary to more oxidizing conditions within a broad pH range (4 13), resulting in a larger aqueous Pu(III) predominance region in the presence of EDTA as opposed to in the absence of EDTA. The subsequent addition of calcium to the Pu EDTA system (Fig. A1c) shifts the aqueous Pu(III)/Pu(IV) boundary to more reducing conditions at $pH_m \geq 7$, slightly decreasing the aqueous Pu(III) predominance region as compared to the region in the absence of calcium. However, the aqueous Pu(III) predominance region in the presence of both EDTA and calcium is still larger than that in the absence of EDTA and calcium, indicating that even with calcium competition, EDTA changes the redox borderline between aqueous Pu(III) and Pu(IV) and increases the stability field of Pu(III) in solution.

Additional changes to Pu(III) and Pu(IV) predominance regions are observed for plutonium solid phases (Fig. 1). Upon the addition of calcium into the system, the Pu(III) solid phase predominance region increases; the $Pu(OH)_3$(am) predominance boundary shifts to significantly lower pH ($pH \geq 8$) in the presence of both 1 mM EDTA and 20 mM $CaCl_2$ as compared to the predominance region in the absence of calcium with 1 mM EDTA ($pH \geq 11$). Similarly, the Pu(IV) solid phase predominance region also increases upon the inclusion of calcium in the calculations by shifting the lower boundary to more reducing conditions from $pH \approx 3$ 8. From these calculations, it is clear that both EDTA and calcium presence can significantly impact the redox boundary between both aqueous and solid Pu(III) and Pu(IV) phases.

Experimentally determined pH_m and pe values are plotted on the Pourbaix diagrams of plutonium in Fig. 1 together with calculated predominance fields of plutonium solid compounds and aqueous species at different total calcium concentrations ($[Ca]_{tot}$) and 1 mM total EDTA concentration ($[EDTA]_{tot}$).

The comparison of experimental pH_m and pe measurements with thermodynamic calculations in Pourbaix diagrams predicts different redox speciation for samples under alkaline ($pH_m > 8$, absence and presence of calcium) and acidic ($pH_m < 6$, only in the absence of calcium) conditions (Fig. 1c). In alkaline systems, the predominance of aqueous Pu(IV) species is predicted, either as Pu(IV) OH EDTA ternary complexes (samples in the absence of calcium) or as $Pu(OH)_4$(aq) (samples in the presence of calcium). Solubility samples equilibrated under acidic conditions fall within the stability field of Pu(III) (with the predominance of the complex $Pu(III)(EDTA)^-$), indicating that reductive dissolution of PuO_2(ncr,hyd) is expected to take place under these conditions. Note, however, that the pe values in the absence of any redox buffer (red squares in Fig. 1) are considered less reliable and may not represent the real redox conditions of the system. Fig. 1 shows also that full dissolution of PuO_2(ncr,hyd) should be expected for the solubility samples equilibrated in acidic conditions, at least those containing HQ for which reliable (pe + pH_m) values are measured.

4.2. Solid and aqueous phase characterization by X ray absorption spectroscopy

Fig. 2 shows the XANES Pu L_{III} edge absorption spectra for selected solid and aqueous phases, together with reference spectra of $Pu(OH)_3$(am) and PuO_2(ncr,hyd) solid phases (Tasi et al., 2018c) and $Pu(III)_{aq}$ and $Pu(IV)_{aq}$ aqueous phases (Brendebach et al., 2009). Table A5 summarizes the energies of the white line (WL) peaks and shifts in the XANES spectra of all samples and references. A comparison of the XANES spectra collected for the two solid phase samples with reference spectra shows that plutonium remained in the +IV oxidation state and no apparent solid phase transformation occurred at either acidic or alkaline pH. In both cases, white line and first feature positions are in excellent agreement with the data reported for $Pu(IV)O_2$(ncr,hyd), considering the typical energy calibration error (±0.5 eV).

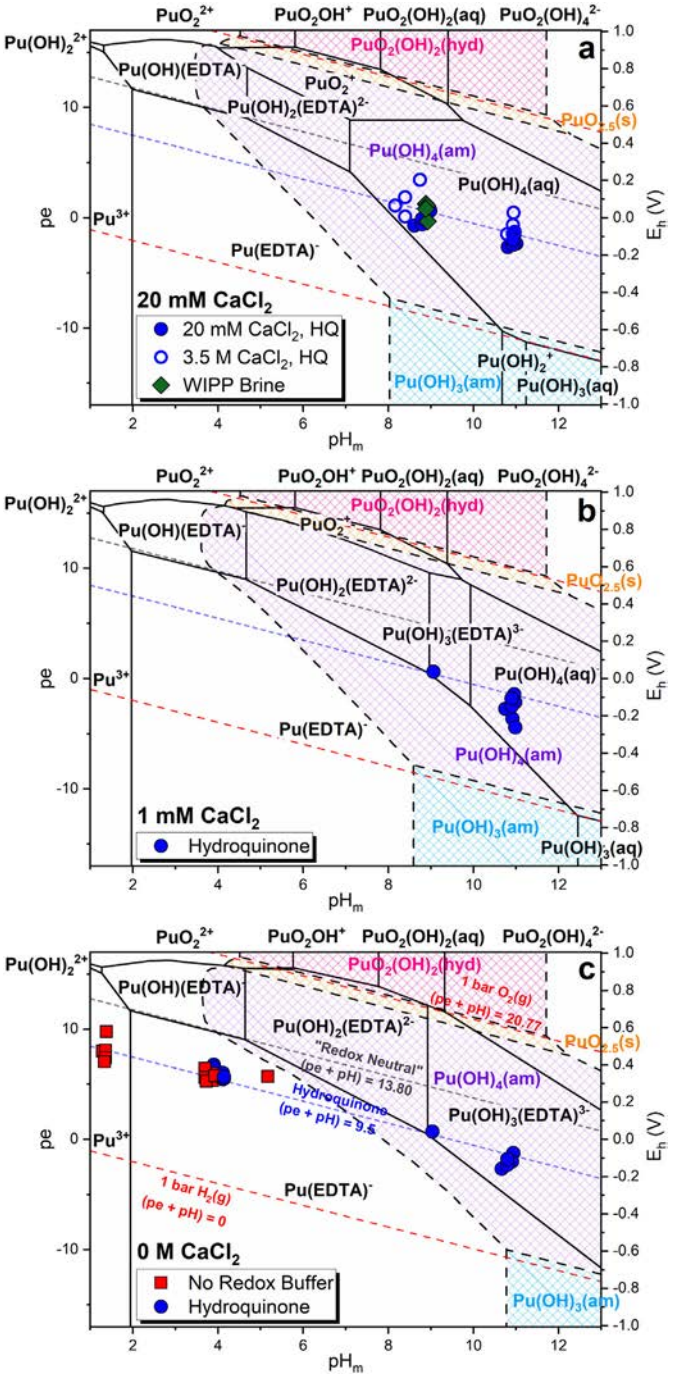

Fig. 1. Pourbaix diagrams of the Pu-EDTA system calculated from Table A1 values at [Pu] = 4·10 ^{4} M, [EDTA] = 1 mM, I = 0.1 M, and (a) 20 mM $CaCl_2$, (b) 1 mM $CaCl_2$, or (c) 0 M $CaCl_2$. Experimental pH_m and pe measurements are shown for experiments conducted in the absence of any redox buffer (solid red squares), in the presence of hydroquinone at 0–20 mM $CaCl_2$ (solid blue circles), in the presence of hydroquinone at 3.5 M $CaCl_2$ (open blue circles), and in the absence of hydroquinone in the WIPP simulated brine (solid green diamonds). Solid black lines correspond to redox borderlines between aqueous plutonium species and dashed black lines represent redox borderlines between solid plutonium species. The borderlines of the stability field of water at (pe + pH_m) = 20.77 and 0 (red dashed lines), the redox neutral line at (pe + pH_m) = 13.80 (gray dashed line) and the line established by hydroquinone at (pe + pH_m) = 9.5 (blue dashed line) are shown for comparison. (For interpretation of the references to colour in this figure legend, the reader is referred to the web version of this article.)

Pu L_{III} edge XANES spectra were collected for supernatant solutions of selected batch samples at $pH_m \leq 6$. Measurements at higher pH_m values were not possible due to the low concentrations of plutonium in the aqueous phase of these experiments. As observed for the solid phases, the comparison of the XANES spectra collected for aqueous phases, white line locations and first feature positions (Table A5) to the reference spectra for $Pu(III)_{aq}$ and $Pu(IV)_{aq}$ from Brendebach et al. (2009) shows that the +IV oxidation state prevails at $4 \leq pH_m \leq 6$ for at least 41 days. Concurrent Vis NIR analyses (Fig. A2) displayed peaks at 504 nm and 495 nm that are consistent with Pu(IV) EDTA complex formation (AlMahamid et al., 1996; Cauchetier and Guichard, 1973; DiBlasi et al., 2021; Meyer et al., 2007). However, the XANES spectrum collected for the $pH_m = 1$ sample exhibited shifts of ~1 eV towards lower energy for both the white line and first feature, indicating partial presence of the +III oxidation state of plutonium. While Pu(IV) still predominates in this sample, it is clear that partial reduction has occurred in the aqueous phase. Vis NIR analyses provide supporting evidence for this result through the minor presence of a Pu(III) peak at 601 nm (Altmaier et al., 2019; Clark et al., 2010; DiBlasi et al., 2021). Spectroscopic data collected for samples equilibrated under acidic conditions are not consistent with experimental pe and pH_m measurements and thermodynamic calculations (see Fig. 1), which predict the predominance of Pu(III) aqueous complexes at all $pH_m < 6$, instead of Pu(IV) predominance in $4 \leq pH_m \leq 6$ samples and partial presence of Pu(III) observed for $pH_m = 1$ samples. Further evidence on this discrepancy is discussed in the following sections.

Fig. A3 shows the Fourier transformed (FT) representation of k^2 weighted EXAFS data for solid phases recovered from a system at pH_m 4 in the absence of calcium and a system at pH_m 9 in the presence of hydroquinone and 20 mM $CaCl_2$. Each dataset was fit with two coordination shells. The first shell at around 1.75 Å (R Δ) corresponds to plutonium bonding to bridging oxygen atoms and oxygen from terminal water and hydroxide units. The second shell at around 3.1 Å (R Δ) corresponds to single scattering from plutonium neighbors within the solid precipitate. All fitting ranges and generated parameters are listed in Table 1.

Evaluation of the EXAFS spectra collected for the solids investigated in this work resulted in coordination numbers of $N_O \approx 5$ and $N_{Pu} \approx 10$ and distances $R_{Pu-O} \approx 2.31$ Å and $R_{O-O} \approx 3.82$ Å. Distances R_{Pu-O} and R_{O-O} determined in this study are in line with data reported for ideal fluorite type PuO_2 ($R_{Pu-O} = 2.32$ Å, $R_{Pu-Pu} = 3.81$ Å), whereas coordination numbers are smaller than those reported for the ideal crystalline material ($N_O = 8$; $N_{Pu} = 12$) (Conradson et al., 2003; Tasi et al., 2018c). An in depth study of this solid phase in the Pu ISA system by Tasi et al. (2018a) resulted in similar structural parameters (i.e., $R_{Pu-O} = 2.30$ Å, $N_O \approx 6$; $R_{Pu-Pu} = 3.80$ Å, $N_{Pu} \approx 4$). The latter study argued that the nanocrystalline nature of the PuO_2(ncr,hyd) solid phase resulted in distorted local order around plutonium centers, which can reduce the coordination number reported for ideal fluorite type PuO_2 due to the destructive interference of the backscattered photoelectron waves. Additionally, fixing $S_0^2 = 1.0$ can lead to slight underestimation of coordination numbers during fitting. These results provide evidence that the initial PuO_2(ncr,hyd) solid phase remains stable throughout the lifetime of the batch experiments and thus controls the solubility of plutonium in the presence of EDTA and calcium.

4.3. Undersaturation solubility experiments in the presence of EDTA and calcium

Fig. 3 shows experimental concentrations of plutonium ($m(Pu)_{tot}$) in equilibrium with PuO_2(ncr,hyd) in solutions containing 1 mM EDTA and $0 \leq [CaCl_2] \leq 3.5$ M or the WIPP simulated brine. The calculated solubility of Pu(IV) species from a PuO_2(am,hyd) solid phase in the absence and in the presence of 1 mM EDTA is provided for comparison as a function of calcium concentration. Steady state was achieved after 6 27 days for experiments in the absence of calcium, 27 53 days for 1 mM 3.5 M $CaCl_2$ experiments, and after 25 days for WIPP simulated brine experiments. Experimental solubility data in all investigated systems are clearly above the calculated solubility of PuO_2(am,hyd) in the absence

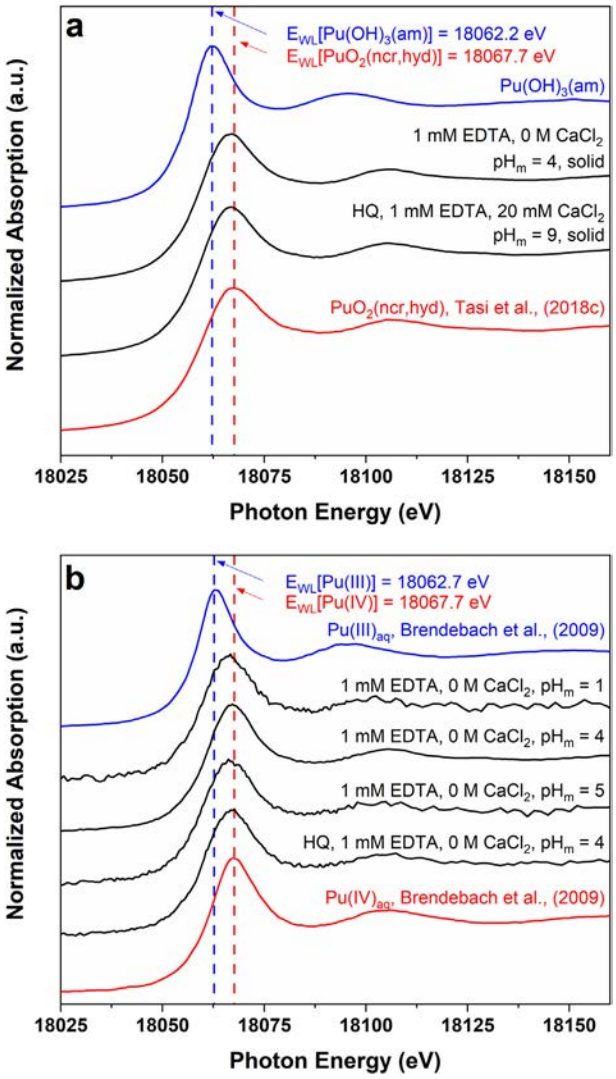

Fig. 2. Pu L_{III}-edge XANES spectra measured in-situ for (a) solid phases or (b) aqueous phases from selected experiments containing PuO_2(ncr,hyd) equilibrated in solutions with 1 mM EDTA and $I = 0.1$ M for 41 days (additional experimental details listed in figure). The spectra of the references for $Pu(IV)_{aq}$ and PuO_2(ncr,hyd) solid phase (red lines) reported in Brendebach et al. (2009) and Tasi et al. (2018c), respectively, $Pu(III)_{aq}$ reported in Brendebach et al. (2009), and freshly synthesized $Pu(OH)_3$(am) solid phase (blue lines) are shown for comparison. (For interpretation of the references to colour in this figure legend, the reader is referred to the web version of this article.)

of EDTA (black line in Fig. 3), thus supporting the predominance of Pu (IV) EDTA complexes in the aqueous phase. Solubility data in the pres ence of EDTA and absence of calcium qualitatively follow the trend of the calculated solubility of Pu(IV) species as a function of pH under the same boundary conditions (blue line in Fig. 3a). This agreement sup ports the expected formation of ternary Pu(IV) OH EDTA complexes as described by Rai et al. (2008). However, experimental values of $m(Pu)_{tot}$ are systematically 1 to 1.5 $\log_{10}$ units lower than the corresponding cal culated solubility. This mismatch between experimental data and ther modynamic calculations may be caused by the following points: (i) overestimation of the stability constants for the formation of the ter nary species or (ii) deviation in the solubility products of the solid phases utilized in each study. For further details, see Section 4.4.

The Pourbaix diagrams shown in Fig. 1 predict the predominance of Pu(III) EDTA aqueous complexes in all acidic samples. For this reason, solubility calculations assuming the reductive dissolution of PuO_2(am, hyd) at $(pe + pH_m) = 9$, including all Pu(IV) OH EDTA and Pu(III) EDTA complexes listed in Table A1, were also conducted and are plotted as a gray line in Fig. 3a. The redox condition $(pe + pH_m) = 9$ for these calculations was selected based off of the experimentally measured pH and pe values. These calculations largely overestimate the experi mental solubility in the presence of EDTA and absence of calcium and are not able to explain the trends in the solubility observed with in creasing pH_m. In agreement with the spectroscopic observations sum marized in Section 4.2, solubility data underpin the predominance of Pu(IV) EDTA aqueous complexes within the investigated systems.

In the presence of EDTA and calcium, thermodynamic calculations predict a clear decrease of the solubility of plutonium with increasing calcium concentrations (green and red lines in Fig. 3b). These predic tions are not reproduced by our experimental data, which show consis tent and systematically higher plutonium concentrations at both $pH_m \approx 9$ and 11 (red and green symbols in Fig. 3b). These observations provide indirect evidence on the possible formation of quaternary Ca Pu(IV) OH EDTA complexes. We note that the predominance of the anionic complexes $Pu(OH)_2(EDTA)^{2-}$ and $Pu(OH)_3(EDTA)^{3-}$ under alkaline conditions represents an appropriate ground for strong ionic interac tions with Ca^{2+} present in solution. Solubility data in the presence of 1 mM and 20 mM $CaCl_2$ follow a close to pH_m independent trend, thus pointing to a solubility equilibrium that involves no exchange of protons.

Rai and co workers also observed higher plutonium concentrations than those predicted by thermodynamic calculations in systems con taining both EDTA and calcium (Fig. 9 in Rai et al. (2008)). Although the authors did not propose any hypothesis to explain such disagree ment, these results provide independent support for the formation of quaternary Ca Pu(IV) OH EDTA complexes.

Experiments conducted at high ionic strength (3.5 M $CaCl_2$ and WIPP brine) exhibit systematically higher plutonium concentrations than those predicted by thermodynamic calculations conducted for EDTA free systems (Fig. 3b). Considering the large excess of calcium in the 3.5 M $CaCl_2$ system and the high stability of the Ca EDTA complex ($\log \beta^\circ_{1,1} = (12.69 \pm 0.06)$), these observations can be only explained by the formation of quaternary Ca Pu(IV) OH EDTA complex(es). Similar to dilute systems, solubility data of plutonium in 3.5 M $CaCl_2$ solutions with $pH_m \approx 9$ and 11 follow pH_m independent behavior. This observa tion points again to a solubility equilibrium involving no exchange of protons.

Table 1
Data range and parameters generated by least-squares fitting of EXAFS spectra.

Sample	k-range (Å ^{1}) fit range (Å)	Shell	N	R (Å)	ΔE_o (eV)[a]	σ^2 (Å^2)	r-factor (%)
$pH_m = 4$	2.7–7.0	O	5.2	2.30	4.37	0.0082	0.3
[EDTA] = 1 mM	1–4	Pu	10.0	3.82		0.0220	
$[Ca]_{tot} = 0$ M							
$pH_m = 9$, HQ	2.7–8.2	O	5.4	2.31	3.94	0.0077	0.5
[EDTA] = 1 mM	1.1–3.9	Pu	9.4	3.82		0.0220	
$[Ca]_{tot} = 20$ mM							

$S_0^2 = 1.0$ fixed (slightly underestimating N in all fits); Errors: $R_{Pu\ O}$ 0.02 Å, $R_{Pu\ Pu}$ 0.02 Å.
[a] Global parameter for both shells.

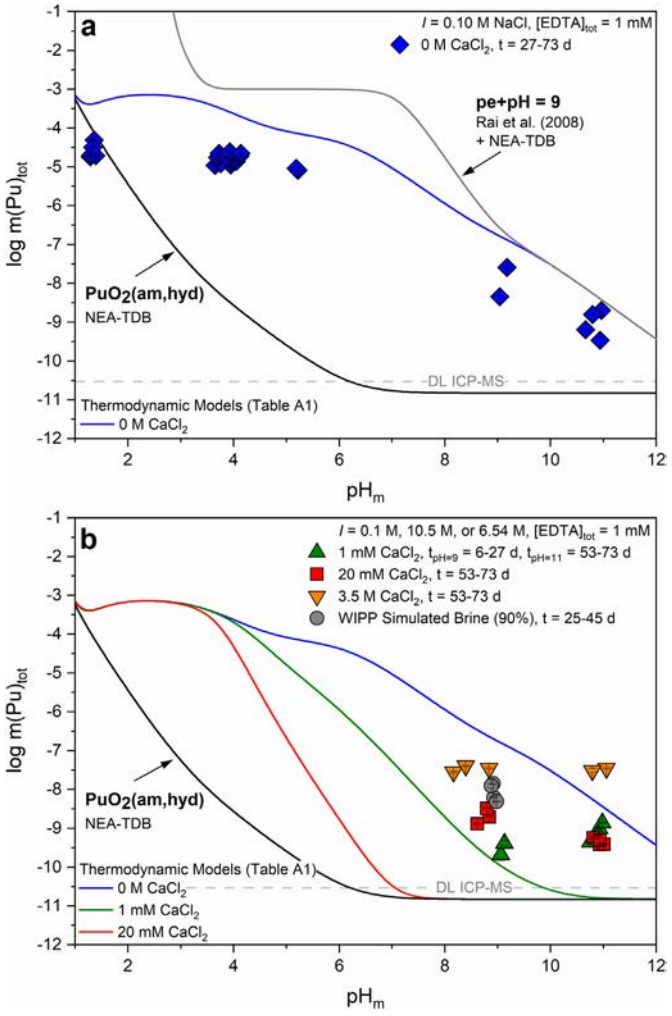

Fig. 3. Experimentally measured $m(Pu)_{tot}$ in equilibrium with PuO_2(ncr,hyd) at $[EDTA]_{tot} = 1$ mM and $I = 0.1$ M NaCl (except 3.5 M $CaCl_2$ and WIPP brine) with (a) 0 M $CaCl_2$ (blue diamonds) and (b) 1 mM $CaCl_2$ (green triangles), 20 mM $CaCl_2$ (red squares), 3.5 M $CaCl_2$ (orange triangles), or WIPP simulated brine (gray circles). Solid and dotted lines correspond to the thermodynamically calculated solubility of PuO_2(am,hyd) under different solution conditions based on the values in Table A1. Gray dashed lines represent the ICP-MS detection limits for the experimental analyses and all error bars are contained within data symbols. (For interpretation of the references to colour in this figure legend, the reader is referred to the web version of this article.)

4.4. Thermodynamic modeling

Datasets of Pu(IV) solubility in the presence of EDTA and absence of calcium determined in this work and reported by Rai et al. (2008) show consistent trends across the entire pH range, but hold a systematic offset in the concentration of plutonium of about 1.5 $\log_{10}$ units (Fig. 3). These observations give support to a consistent aqueous speciation in both studies, while likely reflecting differences in the PuO_2(s) solid phase controlling the solubility. The solid phase used in the present work (PuO_2(ncr,hyd) aged for ca. 11 years) was extensively characterized in a previous study (Tasi et al., 2018c), and the solubility product was determined to be $\log {}^{\circ}K_{s,0} = -(58.1 \pm 0.3)$. This value is in excellent agreement with the NEA TDB selection for an aged amorphous phase PuO_2(am,hyd) (i.e., $\log {}^{\circ}K_{s,0} = -(58.33 \pm 0.52)$).

In contrast, Rai and co workers used a freshly precipitated solid phase, which was aged for ca. 2 h before equilibrating in solutions containing EDTA for up to 91 days (Rai et al., 2001, 2008). Note, however, that the thermodynamic model reported by Rai and co workers (both in the 2001 and 2008 papers) was derived on the basis of the solubility data at t = 7 days. The authors did not characterize the solubility product of this solid phase, and instead used thermodynamic data reported in the literature. In their first publication, Rai and co workers used $\log {}^{\circ}K_{s,0} = -56.85$ for the interpretation of their solubility data (Rai et al., 2001). This value is in line with a solubility constant often assigned in the literature to the amorphous phase $Pu(OH)_4$(am) (i.e., $\log {}^{\circ}K_{s,0} = -(56.8 \pm 1.3)$; see ThermoChimie TDB, Giffaut et al. (2014); originally reported in Lemire and Garisto (1989). However, in 2008, Rai and co workers reinterpreted their solubility using the solubility product associated with the PuO_2(am,hyd) solid phase selected in the NEA TDB, and accordingly obtained complexation constants for the ternary system Pu(IV) OH EDTA that are ~1.5 $\log_{10}$ units higher than those reported by the same authors in 2001. Considering the identical relative stability of the forming species (i.e., the trend of $m(Pu)_{tot}$ as a function of pH_m is the same in both solubility studies (this work; Rai et al., 2001)) and accounting for the well characterized $\log {}^{*}K^{\circ}_{s,0}$ of the solid phase in our solubility study, it follows that the solubility constant used in Rai et al. (2008) is not representative of a freshly precipitated solid phase. Hence, the reason for the offset observed between our experimental data and thermodynamic calculations using the model reported in Rai et al. (2008) is the solubility product used in the latter publication, which underestimates the solubility of plutonium in the absence of EDTA and consequently leads to the overestimation of the equilibrium constants for the Pu(IV) OH EDTA complexes. To address these discrepancies, the following modeling strategy was considered:

(i) all solubility datasets obtained in this work and reported in Rai et al. (2001) were combined for the evaluation performed in the present work;
(ii) conditional solubility constants related to the formation of the ternary hydroxo species determined in Rai et al. (2008) were kept constant (e.g., PuO_2(am,hyd,fresh) + $EDTA^{4-}$ + (4 x)H^+ ⇔ $Pu(OH)_x(EDTA)^{x-}$ + (2 x)H_2O(l), with $\log {}^{*}K'_{s,(1,x,1)}$ (see Table 2); and
(iii) the solubility constant of the freshly precipitated solid phase applied in the experiments of Rai et al. (2001) was readjusted by recalculating the overall stability constants of the given ternary species ($\log \beta$ values, corresponding to the general equation Pu^{4+} + $EDTA^{4-}$ + (x)H_2O(l) ⇔ $Pu(OH)_x(EDTA)^{x-}$ + xH^+, with x = 1, 2 and 3 to gain the best fit on all data sets.

Solubility calculations using this new thermodynamic model are shown in Fig. 4, confirming that the updated model is able to satisfactorily explain the two independent datasets, and a direct comparison of the model description of our experimental data before and after reevaluation can be found in Fig. A5. The resulting thermodynamic constants are summarized in Table 2, which also includes the solubility constant derived in this work for the freshly precipitated solid phase used by Rai et al. (2001). Solubility constants $\log {}^{*}K'_{s,(1,x,1)}$ derived in this work for the Pu(IV) OH EDTA system are approximately 1.2 $\log_{10}$ units lower than those reported in Rai et al. (2008).

Experimental solubility data in the presence of EDTA and calcium cannot be explained without claiming the formation of a quaternary Ca Pu(IV) OH EDTA complex (see discussion in Section 4.3) with the general formula $Ca_xPu(OH)_y(EDTA)_z^{(4+2x-y-4z)}$. Although the experimental dataset for this quaternary system is limited (only two pH_m values and two calcium concentrations), we attempted to derive a preliminary thermodynamic model for this system. Taking the solubility and complexation model discussed above as the basis for the ternary Pu(IV) OH EDTA system, solubility data collected in the presence of EDTA and calcium were fitted to include quaternary $CaPu(OH)_y(EDTA)^{(2-y)}$ complexes with Pu:OH ratios of 1:1, 1:2, 1:3, and 1:4 (i.e., y = 1 4). Although different stoichiometries of EDTA and calcium within the complex may also apply, the number of EDTA (z) and calcium (x) molecules/atoms in the complex was set to 1. This choice was made for the sake of simplicity, but also considering that Coulomb

Table 2
Comparison of solubility constants for Pu(IV) hydrous oxides and equilibrium constants for the formation of ternary Pu(IV)-OH-EDTA complexes as reported in Rai et al. (2008), Boukhalfa et al. (2004), or Rai et al. (2001) to solubility and formation constants derived in this work.

Reaction	log $K°$ or $\beta°$ This work	log $K°$ or $\beta°$ Rai et al. (2008)	log $K°$ or $\beta°$ Boukhalfa et al. (2004)	log $K°$ or $\beta°$ Rai et al. (2001)
$PuO_2(am,hyd) + 2H_2O(l) \Leftrightarrow Pu^{4+} + 4OH$	$-(58.33 \pm 0.52)^a$	$-(58.33 \pm 0.52)^a$		56.85
$PuO_2(am,hyd,fresh)^b + 2H_2O(l) \Leftrightarrow Pu^{4+} + 4OH$	$-(57.15 \pm 0.50)^c$			
$PuO_2(am,hyd,fresh)^b + EDTA^4 + 3H^+ \Leftrightarrow Pu(OH)(EDTA) + H_2O(l)$	$(21.855 \pm 0.292)^d$	$(21.855 \pm 0.292)^e$		$(21.58 \pm 0.35)^e$
$PuO_2(am,hyd,fresh)^b + EDTA^4 + 2H^+ \Leftrightarrow Pu(OH)_2(EDTA)^2$	$(16.871 \pm 0.292)^d$	$(16.871 \pm 0.292)^e$		$(15.92 \pm 0.35)^e$
$PuO_2(am,hyd,fresh)^b + EDTA^4 + H^+ + H_2O(l) \Leftrightarrow Pu(OH)_3(EDTA)^3$	$(7.354 \pm 0.292)^d$	$(7.354 \pm 0.292)^e$		$(6.95 \pm 0.35)^e$
$Pu^{4+} + EDTA^4 + H_2O(l) \Leftrightarrow Pu(OH)(EDTA) + H^+$	$(23.00 \pm 0.30)^f$	(24.203 ± 0.292)	$(25.17 \pm 0.86)^g$	(22.44 ± 0.35)
$Pu^{4+} + EDTA^4 + 2H_2O(l) \Leftrightarrow Pu(OH)_2(EDTA)^2 + 2H^+$	$(18.02 \pm 0.30)^f$	(19.220 ± 0.292)	$(18.03 \pm 0.1)^g$	(16.78 ± 0.35)
$Pu^{4+} + EDTA^4 + 3H_2O(l) \Leftrightarrow Pu(OH)_3(EDTA)^3 + 3H^+$	$(8.50 \pm 0.30)^f$	(9.705 ± 0.292)		(7.80 ± 0.35)

[a] As selected by the NEA-TDB, Guillaumont et al. (2003).
[b] The notation PuO_2(am,hyd,fresh) is assigned in this work to the freshly precipitated solid phase used in the solubility study by Rai et al. (2001). A similar nomenclature is used in the NEA-TDB books referring to freshly precipitated solid phases of tetravalent elements, e.g. ThO_2(am,hyd,fresh) or TcO_2(am,hyd,fresh) (Grenthe et al., 2020; Rand et al., 2008).
[c] Derived in this work from solubility data in Rai et al. (2001).
[d] Taken as reported from Rai et al. (2008). These log $K°_{s,(1,x,1)}$ values were not modified during the model reevaluation.
[e] As detailed in Rai et al. (2008), the primary difference between Rai et al. (2008) and Rai et al. (2001) values was the implementation of acidity constants for EDTA sourced from the NEA-TDB within Rai et al. (2008) calculations. For this reason, Rai et al. (2008) values were implemented within this work.
[f] Derived from experimental data obtained in this work and reported in Rai et al. (2001) as described in the text.
[g] Values corrected to $I = 0$ with the SIT model by Rai et al. (2008).

repulsion is likely to prevent the coordination of a second $EDTA^{4-}$ ion to a highly hydrolyzed Pu(IV) central atom. Results of the different model ing attempts are summarized in Table A6, where the quality parameter represents the averaged square root of the sum of differences between the experimental and calculated plutonium concentrations, calculated as: $[\sum(\log [Pu]_{exp} \log [Pu]_{calc})^2]^{1/2}\cdot(n-1)^{-1}$ (where n is the number of data points). The best fit was obtained assuming the formation of the $CaPu(OH)_4(EDTA)^{2-}$ complex, with log ${}^*K°_{s,(1,1,4,1)} = (6.6 \pm 0.5)$ and log ${}^*\beta°_{(1,1,4,1)} = (8.9 \pm 0.1)$ for the solubility/complexation reac tions PuO_2(ncr,hyd) + Ca^{2+} + $EDTA^{4-}$ + $2H_2O(l) \Leftrightarrow CaPu(OH)_4(EDTA)^{2-}$ and $Ca^{2+} + Pu^{4+} + EDTA^{4-} + 4H_2O(l) \Leftrightarrow CaPu(OH)_4(EDTA)^{2-} + 4H^+$, respectively. Apart from the numerical proof, it also appears to be evident from the nearly constant total plutonium concen trations in solutions with 1 mM and 20 mM $CaCl_2$, that this seemingly pH independent trend in the data (see Fig. 5) can only be represented by assuming the formation of a species with a Pu:OH ratio of 1:4. A di rect comparison of the model with and without quaternary complex in clusion can be found in Fig. A6. The lack of SIT or Pitzer ion interaction coefficients of the anionic species with Ca^{2+}, Mg^{2+}, or Na^+ hinders the proper assessment of plutonium solubility for this system in concen trated brines, but again, the formation of a quaternary complex with a Pu:OH ratio of 1:4 is consistent with the given trend in the data ob served in 3.5 M $CaCl_2$ solutions. This fitting exercise resulted in a tenta tive formula of $CaPu(OH)_4(EDTA)^{2-}$ for the quaternary complex, which is implemented throughout the rest of this discussion. However, further experimentation is required to define the precise stoichiometry of the quaternary Ca Pu(IV) OH EDTA complex(es).

There is increasing evidence in the literature on the formation of ter nary and quaternary complexes of actinides with organic/inorganic li gands involving the interaction of Ca^{2+} with a negatively charged central moiety (Bernhard et al., 1996; Endrizzi and Rao, 2014; Fellhauer et al., 2010, 2016; Kalmykov and Choppin, 2000; Lee and Yun, 2013; Neck et al., 2009; Rojo et al., 2021; Tasi et al., 2018b; Tits et al., 2005; Vercammen et al., 2001; among others). The best approach to assess the stability of these complexes requires the definition of a chemical reaction involving the aqueous species prevailing in solution. For the systems Ca U(VI) CO_3 (Endrizzi and Rao, 2014), Ca Pu(IV) ISA (Tasi et al., 2018b), and Ca Np(V) OH (Fellhauer et al., 2016), the fol lowing equilibrium reactions can be accordingly defined:

$$Ca^{2+} + UO_2(CO_3)_3^{4} \Leftrightarrow CaUO_2(CO_3)_3^{2} \quad \log K° \quad (5.15 \pm 0.06) \qquad (1)$$

$$Ca^{2+} + CaUO_2(CO_3)_3^{2} \Leftrightarrow Ca_2UO_2(CO_3)_3(aq) \quad \log K° \quad (3.85 \pm 0.06) \qquad (2)$$

$$Ca^{2+} + Pu(OH)_4ISA \Leftrightarrow CaPu(OH)_4ISA^+ \quad \log K° \quad (3.37 \pm 0.16) \qquad (3)$$

$$Ca^{2+} + Pu(OH)_5ISA^2 \Leftrightarrow CaPu(OH)_5ISA(aq) \quad \log K° \quad (4.22 \pm 0.15) \qquad (4)$$

$$Ca^{2+} + NpO_2(OH)_2 \Leftrightarrow CaNpO_2(OH)_2^{+} \quad \log K° \quad (2.9 \pm 0.5) \qquad (5)$$

A key difference between the ternary/quaternary systems described above and the Ca Pu(IV) EDTA system is the stability of the binary com plexes CaL, where $L = CO_3^{2-}$ ($\log \beta°_{(1,1)} = 3.22$), ISA^- ($\log \beta°_{(1,1)} = 1.7$), OH^- ($\log \beta°_{(1,1)} = 1.22$), or $EDTA^{4-}$ ($\log \beta°_{(1,1)} = 12.69$). In this con text, reactions (6) and (7) can be proposed to describe the chemical equilibrium involving the species predominant in solution for the Ca Pu(IV) EDTA system. Assuming an excess of calcium in the system, the large stability of the $Ca(EDTA)^{2-}$ complex induces a significant drop in $[EDTA^{4-}]_{free}$ available for complexation with Pu(IV), eventually favoring the prevalence of reaction (7):

$$Ca^{2+} + Pu(OH)_4(EDTA)^4 \Leftrightarrow CaPu(OH)_4(EDTA)^2 \qquad (6)$$

$$Ca(EDTA)^2 + Pu(OH)_4(aq) \Leftrightarrow CaPu(OH)_4(EDTA)^2 \qquad (7)$$

The combination of log ${}^*\beta°_{(1,1,4,1)} = (8.9 \pm 0.1)$ determined in this work for the formation of the $CaPu(OH)_4(EDTA)^{2-}$ complex with the equilibrium constants for the formation of $Ca(EDTA)^{2-}$ ($\log \beta°_{(1,1)} = (12.69 \pm 0.06)$) and $Pu(OH)_4(aq)$ (log ${}^*\beta°_{(1,4)} = -(8.5 \pm 0.5)$) allows for the determination of the equilibrium constant for reaction (7): log $K°(7) = (4.7 \pm 0.5)$. The comparison of this equilibrium constant with the values of log $K°(1)$ to log $K°(5)$ listed above gives an additional qual itative insight into the stability of the quaternary complex $CaPu(OH)_4(EDTA)^{2-}$, which is the same order of magnitude as the stability of the $CaPu(OH)_5ISA(aq)$ or $CaUO_2(CO_3)_3^{2-}$ complexes.

Although the precise stoichiometry of the quaternary $CaPu(OH)_4(EDTA)^{2-}$ complex might need to be revisited on the basis of future ex perimental studies, we argue that the predominance of quaternary complex(es) is the most likely explanation for the solubility trends ob served throughout the course of our experiments and is in line with thermodynamic data reported for other ternary/quaternary complexes involving the participation of calcium.

4.5. Relevance of the new species and thermodynamic data for environmental and nuclear waste disposal applications

EDTA concentrations in specific radioactive waste disposal scenarios vary depending on the expected type of waste. High level radioactive

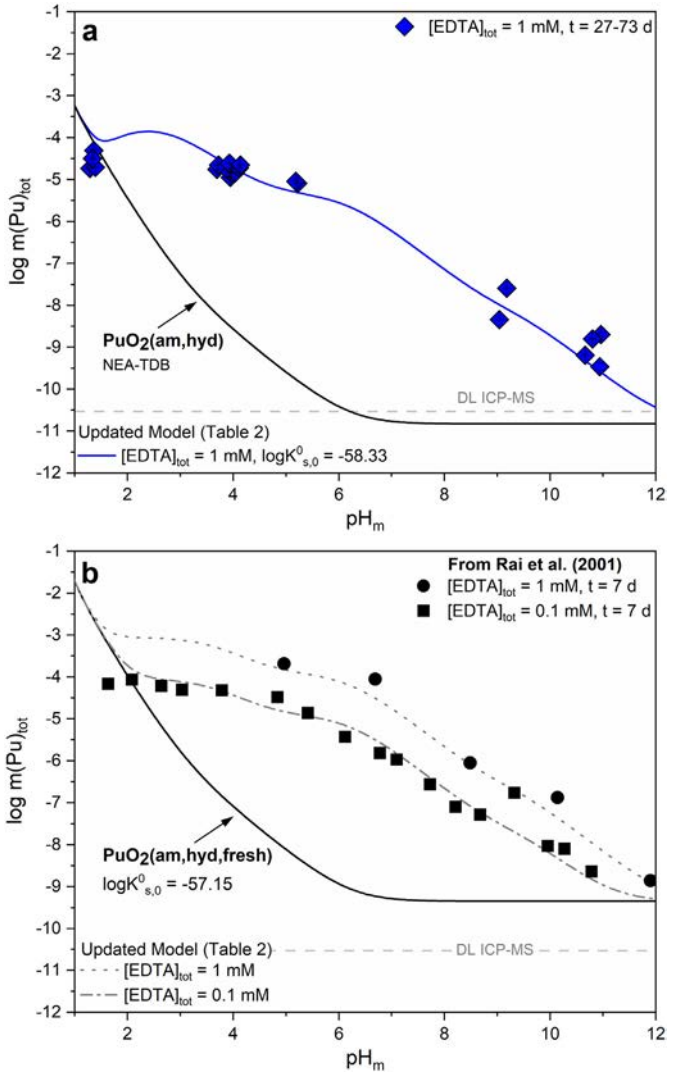

Fig. 4. (a) Experimental PuO_2(ncr,hyd) solubility at equilibrium in 1 mM EDTA solution with 0 M $CaCl_2$ and (b) Rai et al. (2001) solubility data at t = 7 days in 1 mM and 0.1 mM EDTA solutions with 0 M $CaCl_2$ as compared to the calculated solubility using the Pu(IV)-OH-EDTA thermodynamic model derived in this work through the simultaneous fit of both experimental datasets (see text and values in Table 2). Gray dotted lines represent the ICP-MS detection limits for the experimental analyses and all error bars are contained within data symbols.

waste (HLW), which consists of used nuclear fuel or highly radioactive waste materials (i.e., fission products) that remain after fuel reprocessing, is not expected to contain EDTA (Clark and Ewing, 2006; US NRC, 2020). Processes for creation of specific waste forms for HLW, such as vitrification, will destroy any organic components of the waste prior to disposal. Low and intermediate level radioactive waste (LILW), or waste which contains radioactive and nonradioactive components that may adversely affect humans and the environment, can contain EDTA originating from either the waste itself or the waste packaging. The estimated amount of EDTA disposed in the Swedish LILW repository SFR 1 is 10 kg, which equates to a maximum of $3.9{\cdot}10^{-4}$ M total ligand concentrations in different vaults of the repository (Bradbury and Van Loon, 1997; Chapman et al., 2002; Fanger et al., 2001). However, further disposal of EDTA into the facility is prohibited according to new regulations. Compared to current regulations for LILW, the Waste Isolation Pilot Plant (WIPP) in the United States, which is responsible for the deep geologic disposal of defense transuranic waste (TRU), contains large quantities of EDTA; an estimated $4.03{\cdot}10^{2}$ kg of EDTA has been deposited in the WIPP, which translates to $8{\cdot}10^{-5}$ M EDTA accounting for the entire volume of the repository (Appendix SOTERM 2019, 2019). Finally, legacy waste, such as that disposed of at the Hanford Site and Maxey Flats, can also contain EDTA (Cleveland and Rees, 1981; Hakem et al., 2001; McFadden, 1980). The waste tanks at the Hanford Site (Washington, USA) contain ~$3.5{\cdot}10^{8}$ L mixed radioactive wastes generated from more than 40 years of plutonium processing, and this waste is estimated to include ~$8.3{\cdot}10^{4}$ kg EDTA (Campbell et al., 2000; Colburn and Peterson, 2021; Freeman Pollard et al., 1994; Hakem et al., 2001; Rai et al., 2008; Samuels et al., 1994). An analysis of waste from Hanford Tank 241 SY 101 by Campbell et al. (2000) exhibited total organic carbon concentrations of ~2000 ppm, 70 90% of which could be attributed to organic chelators (i.e., primarily EDTA or oxalate); this equates to a maximum total ligand concentration of ~$6{\cdot}10^{-3}$ M within Tank 241 SY 101 at the Hanford Site. Ultimately, it is both appropriate and necessary to consider EDTA in the context of nuclear waste disposal for TRU, LILW, and legacy waste, although the concentrations are expected to vary for each specific disposal situation; herein, we use 0.1 mM EDTA to approximate both environmentally and repository relevant boundary conditions.

Thermodynamic data derived for the ternary Pu(IV) OH EDTA system (Table 2) in combination with the tentative equilibrium constant proposed for the quaternary $CaPu(OH)_4(EDTA)^{2-}$ complex were considered to prepare updated Pourbaix diagrams of plutonium in the presence of EDTA (Fig. 6a) and plutonium in the presence of both EDTA and calcium (Fig. 6b). The updated diagram in Fig. 6a (0 M $CaCl_2$) shows a smaller aqueous Pu(IV) predominance field than previously calculated using the thermodynamic model reported in Rai et al. (2008), which results in an increase of the stability field of aqueous Pu(III) species. This indicates that the dominant valence of plutonium for the acidic experiments reported within this work is still predicted to be Pu(III), even with the inclusion of revised thermodynamic constants within the calculations and suggests that the thermodynamic constants for Pu(III) EDTA species may not be reliable. To address this discrepancy, future experimentation and modeling will focus on reassessing the thermodynamics of the Pu(III) EDTA system. The Pourbaix diagram in Fig. 6b (20 mM $CaCl_2$), while preliminary in nature, displays the overwhelming predominance of the quaternary $CaPu(OH)_4(EDTA)^{2-}$ complex in the presence of both EDTA and calcium under alkaline conditions. The formation of this quaternary complex increases the stability field of Pu(IV) to the detriment of the Pu(III) EDTA region at pH ≥ 6, thus highlighting the specific impact of calcium in the redox distribution of plutonium for systems containing EDTA.

Colored regions in Fig. 6 correspond to the (pe + pH) conditions found in natural waters (groundwater, seawater, rain/streams) and expected in underground repositories for nuclear waste (Duro et al., 2012; Runde, 2000). Fig. 6a and Fig. 6b show that both Pu(IV) EDTA and Pu(III) EDTA complexes have large stability fields within the (pe + pH) conditions prevailing in natural waters (gray shaded area). In contrast to previous assumptions, the ubiquitous presence of calcium in environmental systems does not inhibit the complexation of plutonium with EDTA but rather promotes the stabilization of Pu(IV) in solution through the formation of quaternary complexes. Under the reducing conditions expected in underground repositories (orange colored region), our updated thermodynamic model predicts the coexistence of Pu(IV) EDTA or Pu(III) EDTA complexes over the range of 2 3 pH units. However, the large inventory of calcium in specific repository concepts/conditions (e.g., cementitious systems) is expected to enhance the stability field of Pu(IV), thus shifting the Pu(IV)/Pu(III) redox border towards more reducing conditions.

The discussion above highlights the complexity of quaternary M Pu OH EDTA systems. In our view, the generally accepted outcompetition of Pu EDTA complexation by some environmentally relevant major cations such as calcium may need to be revisited. Experimental evidence collected in this work suggests the possible formation of quaternary complexes of plutonium in these systems. The formation of such complexes may significantly affect the chemical behavior of plutonium in the presence of EDTA under a wide range of geochemical conditions of

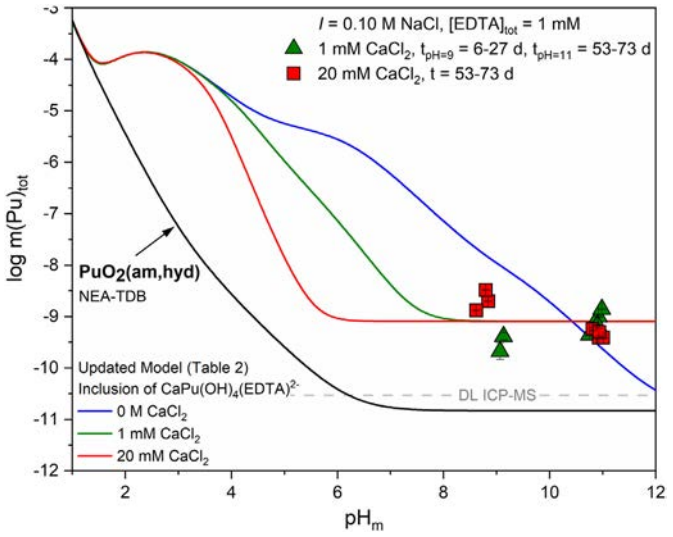

Fig. 5. Experimental PuO_2(ncr,hyd) solubility at equilibrium in 1 mM EDTA solutions with 1 mM or 20 mM $CaCl_2$ as compared to the calculated solubility using the thermodynamic model derived in this work for the Pu(IV)-OH-EDTA system (see Table 2) and including the formation of the quaternary complex $CaPu(OH)_4(EDTA)^{2}$. Gray dotted lines represent the ICP-MS detection limits for the experimental analyses and all error bars are contained within data symbols.

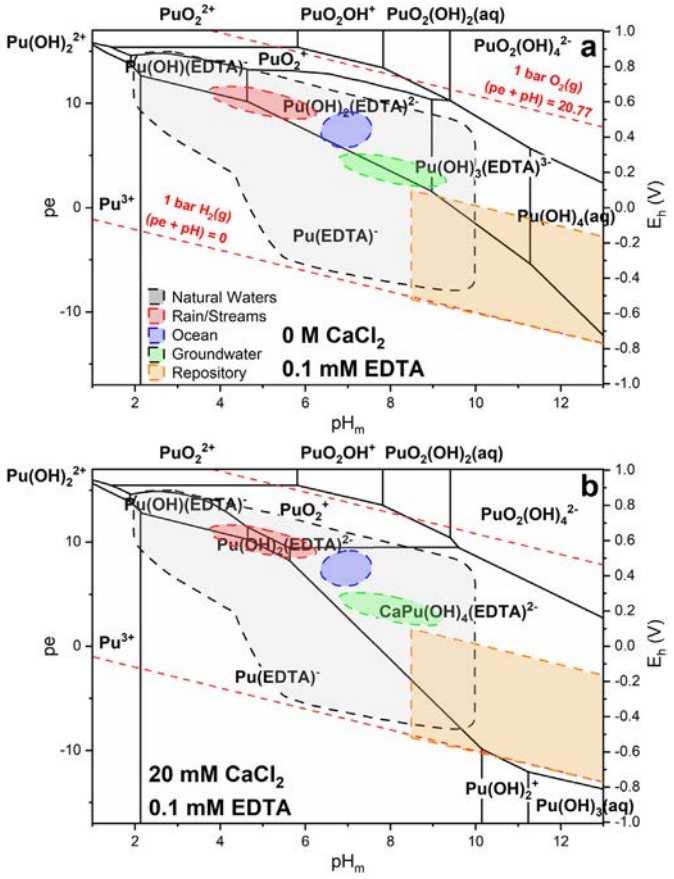

Fig. 6. Pourbaix diagram of the Pu-EDTA system calculated for [Pu] = 1·10 ^{11} M, [EDTA] = 0.1 mM, I = 0.1 M, and (a) 0 M $CaCl_2$ or (b) 20 mM $CaCl_2$ using the reevaluated Pu(IV)-EDTA equilibrium constants in Table 2 and the newly generated log $K^{\circ}_{s,(1,1,4,1)}$ for the quaternary complex. Solid black lines correspond to redox borderlines between aqueous species and colored regions correspond to environmentally- and repository-relevant boundary conditions.

environmental relevance as well as in underground repositories for nu clear waste disposal.

5. Conclusions

Undersaturation solubility experiments using a well characterized PuO_2(ncr,hyd) solid phase and chemically controlled, well defined redox conditions in solution, in combination with advanced spectro scopic techniques, are considered to attain a thermodynamic descrip tion of the Ca Pu(IV) EDTA H_2O system, which includes previously unreported quaternary Ca Pu(IV) OH EDTA complex(es).

Although the current NEA TDB selection does not consider the for mation of hydroxo species for any of the An(IV) EDTA systems, more recent literature provide evidence that these complexes dominate An (IV) aqueous speciation in the presence of EDTA under weakly acidic to hyperalkaline pH conditions. The use of thermodynamic models available in the literature for the Pu(IV) OH EDTA ternary system re sults in a systematic overestimation of the plutonium solubility data de termined in the present study in the absence of calcium. By using the well defined solubility constant available for the solid phase used in this work and by adjusting the solubility product of the solid phase in the work of Rai et al. (2001), solubility data in both studies gave a proper basis for the reevaluation of the overall formation constants (log $\beta^{\circ}_{(1,x,1)}$) for the ternary complexes $Pu(OH)(EDTA)^{-}$, $Pu(OH)_2(EDTA)^{2-}$, and $Pu(OH)_3(EDTA)^{3-}$. This exercise resulted in a consistent thermody namic model that is able to successfully explain both solubility data sets. The comparison of both solubility studies also provides a sound basis for the differentiation between the solubility products of an amorphous, freshly precipitated PuO_2 solid phase and an aged PuO_2 solid phase with higher crystallinity. Following the nomenclature considered in the NEA TDB for the case of Th(IV) (Rand et al., 2008), we propose the definition of the solid phase PuO_2(am,hyd,fresh) with a solubility prod uct of log $K^{\circ}_{s,0} = -(57.15 \pm 0.50)$.

The formation of quaternary Ca Pu(IV) OH EDTA complex(es) is strongly supported by solubility experiments conducted over a wide range of total calcium concentrations ($1\ mM < [Ca(II)]_{tot} < 3.5\ M$). The pH independent trend (i.e., nearly constant total plutonium con centrations quantified in the alkaline range) hinted towards a Pu:OH stoichiometric ratio of 1:4 in the quaternary complex, which is tenta tively defined as $CaPu(OH)_4(EDTA)^{2-}$. As a consequence of the stabilization effect of Ca(II) on the Pu(IV) OH EDTA system, the previ ously defined redox boundary for Pu(III)/Pu(IV) aqueous species suffers a significant shift towards lower (pe + pH) values, increasing the stabil ity field of $Pu(IV)_{aq}$ species under conditions relevant in the context of nuclear waste disposal. However, additional experimental efforts are re quired to conclusively determine the stoichiometry of the quaternary complex and its impact on the Pu(III)/Pu(IV) aqueous redox boundary. In order to properly assess this effect, similar work will also be con ducted with Pu(III) to evaluate the possible formation of stable Ca Pu (III) OH EDTA quaternary complexes.

Beyond the effect of calcium on the Pu(IV) OH EDTA system and in analogy to observations reported for other chelating ligands (e.g., citrate), such stabilization effects may be anticipated for other di and trivalent metal ions. The possible formation of quaternary M(II)/M (III) Pu(IV) OH EDTA complex(es) emphasizes the importance of reinterpreting the role of major cations of environmental relevance (e.g., calcium, iron, magnesium, lead) for defining the speciation and mobility of plutonium under repository and environmentally relevant conditions.

Funding sources

This work was supported by the DOE Scholars Program (sponsored by the U.S. Department of Energy, administered by the Oak Ridge Insti tute for Science and Education, and funded by the WIPP project) and the Institute for Nuclear Waste Disposal (Karlsruhe Institute of Technology).

CRediT authorship contribution statement

Nicole A. DiBlasi: Conceptualization, Methodology, Formal analysis, Investigation, Visualization, Writing original draft, Writing review & editing. **Agost G. Tasi:** Conceptualization, Methodology, Formal analysis, Investigation, Writing review & editing, Supervision. **Xavier Gaona:** Conceptualization, Methodology, Resources, Writing review & editing, Supervision, Project administration, Funding acquisition. **David Fellhauer:** Validation, Writing review & editing, Supervision. **Kathy Dardenne:** Formal analysis, Resources, Writing review & editing, Supervision. **Jörg Rothe:** Formal analysis, Resources, Writing review & editing. **Donald T. Reed:** Conceptualization, Writing review & editing, Project administration, Funding acquisition. **Amy E. Hixon:** Conceptualization, Writing review & editing, Project administration. **Marcus Altmaier:** Conceptualization, Resources, Writing review & editing, Project administration, Funding acquisition.

Declaration of competing interest

The authors declare that they have no known competing financial interests or personal relationships that could have appeared to influence the work reported in this paper.

Acknowledgements

The authors would like to acknowledge Frank Geyer and Cornelia Walschburger at KIT INE for their efforts in the collection of ICP MS results. The KIT Institute for Beam Physics and Technology (IBPT) is acknowledged for the operation of the storage ring, the Karlsruhe Research Accelerator (KARA), and provision of beamtime at the KIT synchrotron light source. This research was supported, in part, by an appointment to the DOE Scholars Program, sponsored by the U.S. Department of Energy, administered by the Oak Ridge Institute for Science and Education, and funded by the WIPP Project (DOE CBFO). The three month internship by N.A. DiBlasi was performed at KIT INE as part of a joint collaboration between KIT INE, the University of Notre Dame, and the Los Alamos Actinide Chemistry and Repository Science program.

References

AlMahamid, I., Becraft, K.A., Hakem, N.L., Gatti, R.C., Nitsche, H., 1996. Stability of various plutonium valence states in the presence of NTA and EDTA. Radiochim. Acta 74, 129–134. https://doi.org/10.1524/ract.1996.74.special-issue.129.

Altmaier, M., Metz, V., Neck, V., Müller, R., Fanghänel, Th., 2003. Solid-liquid equilibria of $Mg(OH)_2$(cr) and $Mg_2(OH)_3Cl{\cdot}4H_2O$(cr) in the system Mg-Na-H-OH-Cl-H2O at 25°C. Geochim. Cosmochim. Acta 67, 3595–3601. https://doi.org/10.1016/S0016-7037(03)00165-0.

Altmaier, M., Neck, V., Fanghänel, T., 2008. Solubility of Zr(IV), Th(IV) and Pu(IV) hydrous oxides in $CaCl_2$ solutions and the formation of ternary Ca-M(IV)-OH complexes. Radiochim. Acta 96, 541–550. https://doi.org/10.1524/ract.2008.1535.

Altmaier, M., Gaona, X., Fellhauer, D., Clark, D.L., Runde, W.H., Hobart, D.E., 2019. Chapter 22. Aqueous solution and coordination chemistry of plutonium. In: Clark, D.L., Geeson, D.A., Hanrahan Jr., R.J. (Eds.), Plutonium Handbook. American Nuclear Society, La Grange Park, IL, USA.

Anderegg, G., Podder, N.G., Bläuenstein, P., Hangartner, M., Stünzi, H., 1975. Pyridine derivatives as complexing agents X. thermodynamics of complex formation of N, N'-bis-(2-pyridylmethyl)-ethylenediamine and of two higher homologues. J. Coord. Chem. 4, 267–275. https://doi.org/10.1080/00958977508075911.

Appendix SOTERM-2019, 2019. Actinide Chemistry Source Term (No. DOE/WIPP-19-3609, Rev. 0), 2019. Title 40 CFR Part 191 Subparts B and C Compliance Recertification Application. United States Department of Energy.

Arena, G., Musumeci, S., Purrello, R., Sammartano, S., 1983. Calcium- and magnesium-EDTA complexes. Stability constants and their dependence on temperature and ionic strength. Thermochim. Acta 61, 129–138. https://doi.org/10.1016/0040-6031(83)80309-8.

Ayres, J.A. (Ed.), 1970. Decontamination of Nuclear Reactors and Equipment. Ronald Press Company, New York, New York.

Berner, U.R., 1992. Evolution of pore water chemistry during degradation of cement in a radioactive waste repository environment. Waste Management, Cementitious Materials in Radioactive Waste Management 12, 201–219. https://doi.org/10.1016/0956-053X(92)90049-O.

Bernhard, G., Geipel, G., Brendler, V., Nitsche, H., 1996. Speciation of uranium in seepage waters of a mine tailing pile studied by time-resolved laser-induced fluorescence spectroscopy (TRLFS). Radiochim. Acta 74, 87–92. https://doi.org/10.1524/ract.1996.74.special-issue.87.

Boukhalfa, H., Reilly, S.D., Smith, W.H., Neu, M.P., 2004. EDTA and mixed-ligand complexes of tetravalent and trivalent plutonium. Inorg. Chem. 43, 5816–5823. https://doi.org/10.1021/ic035484p.

Bradbury, M.H., Van Loon, L.R., 1997. Cementitious Near-field Sorption Data Bases for Performance Assessment of a L/ILW Repository in Palfris Host Rock (No. PSI-98-01). Paul Scherrer Institut, Villigen, Switzerland.

Brendebach, B., Banik, N.L., Marquardt, C.M., Rothe, J., Denecke, M., Geckeis, H., 2009. X-ray absorption spectroscopic study of trivalent and tetravalent actinides in solution at varying pH values. Radiochimica Acta International journal for chemical aspects of nuclear science and technology 97, 701–708. https://doi.org/10.1524/ract.2009.1674.

Bube, C., Metz, V., Bohnert, E., Garbev, K., Schild, D., Kienzler, B., 2013. Long-term cement corrosion in chloride-rich solutions relevant to radioactive waste disposal in rock salt – leaching experiments and thermodynamic simulations. Physics and Chemistry of the Earth, Parts A/B/C, Coupled Physical and Chemical Transformations Affecting the Performance of GeoSystems 64, 87–94. https://doi.org/10.1016/j.pce.2012.11.001.

Campbell, J.A., Mong, G.M., Clauss, S., Sharma, A., Hoppe, E., 2000. Analysis of Hanford Tank Wastes, WM'00 Conference Proceedings.

Cauchetier, P., Guichard, C., 1973. Etude Électrochimique Ét Spectrophotométrique Des Complexes Des Ions Du Plutonium Avec l'EDTA. Radiochim. Acta 19, 137–146. https://doi.org/10.1524/ract.1973.19.3.137.

Cauchetier, P., Guichard, C., 1975. Etude electrochimique et spectrophotometrique des complexes des ions du plutonium avec l'EDTA Plutonium(V) et (VI). J. Inorg. Nucl. Chem. 37, 1771–1778. https://doi.org/10.1016/0022-1902(75)80315-0.

Chapman, N.A., Maul, P.R., Robinson, P.C., Savage, D., 2002. SKB's Project SAFE for the SFR 1 Repository, a Review by Consultants to SKI (No. SKI-R-02/61-SE). Swedish Nuclear Power Inspectorate, Stockholm, Sweden.

Charlton, S.R., Parkhurst, D.L., 2011. Modules based on the geochemical model PHREEQC for use in scripting and programming languages. Comput. Geosci. 37, 1653–1663. https://doi.org/10.1016/j.cageo.2011.02.005.

Ciavatta, L., 1980. The specific interaction theory in evaluating ionic equilibria. Ann. Chim. (Rome) 70, 551.

Clark, S.B., Ewing, R.C., 2006. Panel 5 Report: Advanced Waste Forms, Basic Research Needs for Advanced Nuclear Energy Systems. Office of Science, Department of Energy.

Clark, D.L., Hecker, S.S., Jarvinen, G.D., Neu, M.P., 2010. Plutonium. In: Morss, L.R., Edelstein, N.M., Fuger, J. (Eds.), The Chemistry of the Actinide and Transactinide Elements, the Chemistry of the Actinide and Transactinide Elements. Springer Netherlands, Dordrecht, pp. 813–1264 https://doi.org/10.1007/1-4020-3598-5_7.

Cleveland, J.M., Rees, T.F., 1981. Characterization of plutonium in Maxey flats radioactive trench leachates. Science 212, 1506–1509. https://doi.org/10.1126/science.212.4502.1506.

Colburn, H.A., Peterson, R.A., 2021. A history of Hanford tank waste, implications for waste treatment, and disposal. Environ. Prog. Sustain. Energy 40, e13567. https://doi.org/10.1002/ep.13567.

Conradson, S.D., Begg, B.D., Clark, D.L., Den Auwer, C., Espinosa-Faller, F.J., Gordon, P.L., Hess, N.J., Hess, R., Keogh, D.W., Morales, L.A., Neu, M.P., Runde, W., Tait, C.D., Veirs, D.K., Villella, P.M., 2003. Speciation and unusual reactivity in PuO2+x. Inorg. Chem. 42, 3715–3717. https://doi.org/10.1021/ic026044l.

DiBlasi, N.A., Yalçintas, E., Stanley, F.E., Reed, D.T., Hixon, A.E., 2021. Influence of ethylenediaminetetraacetic acid on the long-term oxidation state distribution of plutonium. Chemosphere 274, 129741. https://doi.org/10.1016/j.chemosphere.2021.129741.

Duro, L., Grivé, M., Domenech, C., Roman-Ross, G., Bruno, J., 2012. Assessment of the Evolution of the Redox Conditions in SFR 1 (Technical Report No. SKB TR-12-12). Svensk Kärnbränslehantering AB, Stockholm, Sweden.

Endrizzi, F., Rao, L., 2014. Chemical speciation of uranium(VI) in marine environments: complexation of calcium and magnesium ions with $[(UO_2)(CO_3)_3]_4$ and the effect on the extraction of uranium from seawater. Chem. Eur. J. 20, 14499–14506. https://doi.org/10.1002/chem.201403262.

Fanger, G., Skagius, K., Wiborgh, M., 2001. Project SAFE. Complexing Agents in SFR (No. SKB-R-01-04). Swedish Nuclear Fuel and Waste Management Co, Stockholm, Sweden.

Felipe-Sotelo, M., Edgar, M., Beattie, T., Warwick, P., Evans, N.D.M., Read, D., 2015. Effect of anthropogenic organic complexants on the solubility of Ni, Th, U(IV) and U(VI). J. Hazard. Mater. 300, 553–560. https://doi.org/10.1016/j.jhazmat.2015.07.060.

Fellhauer, D., Neck, V., Altmaier, M., Lützenkirchen, J., Fanghänel, T., 2010. Solubility of tetravalent actinides in alkaline $CaCl_2$ solutions and formation of $Ca_4[An(OH)_8]^{4+}$ complexes: a study of Np(IV) and Pu(IV) under reducing conditions and the systematic trend in the An(IV) series. Radiochim. Acta 98, 541–548. https://doi.org/10.1524/ract.2010.1751.

Fellhauer, D., Rothe, J., Altmaier, M., Neck, V., Runke, J., Wiss, T., Fanghänel, T., 2016. Np(V) solubility, speciation and solid phase formation in alkaline $CaCl_2$ solutions. Part I: Experimental results. Radiochimica Acta 104, 355–379. https://doi.org/10.1515/ract-2015-2489.

Foreman, J.K., Smith, T.D., 1957a. The nature and stability of the complex ions formed by ter-, quadri-, and sexa-valent plutonium ions with ethylenediaminetetra-acetic acid. Part I. PH titrations and ion-exchange studies. Journal of the Chemical Society (Resumed), 1752–1758 https://doi.org/10.1039/JR9570001752.

Foreman, J.K., Smith, T.D., 1957b. The nature and stability of the complex ions formed by ter-, quadri-, and sexa-valent plutonium ions with ethylenediaminetetra-acetic acid (edta). Part II. Spectrophotometric studies. Journal of the Chemical Society (Resumed), 1758–1762 https://doi.org/10.1039/JR9570001758.

Freeman-Pollard, J.R., Caggiano, J.A., Trent, S.J., Bechtel Hanford Inc., United States Department of Energy, Office of Environmental Restoration and Waste Management, Enserch Environmental Corporation, Hart Crowser Inc., 1994. Engineering Evaluation of the GAO-RCED-89-157, Tank 241-T-106 Vadose Zone Investigation. Bechtel Hanford, Inc., Richland, Wash.

Geckeis, H., Zavarin, M., Salbu, B., Lind, O.C., Skipperud, L., 2019. Environmental chemistry of plutonium. Chemistry, Plutonium Handbook. American Nuclear Society, La Grange Park, IL, USA.

Gel'man, A.D., Moskvin, A.I., Artyukhin, P.I., 1959. Composition and dissociation constants of Pu (V) and Pu (III) complexes with ethylenediaminetetraacetic acid. The Soviet Journal of Atomic Energy 7, 667–668. https://doi.org/10.1007/BF01480347.

Giffaut, E., Grivé, M., Blanc, Ph., Vieillard, Ph., Colàs, E., Gailhanou, H., Gaboreau, S., Marty, N., Madé, B., Duro, L., 2014. Andra thermodynamic database for performance assessment: ThermoChimie. Applied Geochemistry, Geochemistry for Risk Assessment: Hazardous waste in the Geosphere. 49, pp. 225–236. https://doi.org/10.1016/j.apgeochem.2014.05.007.

Gražulis, S., Daškevič, A., Merkys, A., Chateigner, D., Lutterotti, L., Quirós, M., Serebryanaya, N.R., Moeck, P., Downs, R.T., Le Bail, A., 2012. Crystallography open database (COD): an open-access collection of crystal structures and platform for world-wide collaboration. Nucleic Acids Res. 40, D420–D427. https://doi.org/10.1093/nar/gkr900.

Grenthe, I., Gaona, X., Plyasunov, A.V., Rao, L., Runde, W.H., Grambow, B., Konings, R.J.M., Smith, A.L., Moore, E.E., 2020. Second Update on the Chemical Thermodynamics of Uranium, Neptunium, Plutonium, Americium and Technetium, Chemical Thermodynamics. OECD Nuclear Energy Agency, Boulogne-Billancourt, France.

Guillaumont, R., Fanghänel, T., Fuger, J., Grenthe, I., Neck, V., Palmer, D.A., Rand, M.H., 2003. Update on the chemical thermodynamics of uranium. Neptunium, Plutonium, Americium and Technetium, Chemical Thermodynamics. OECD Nuclear Energy Agency, Issy-les-Moulineaux, France.

Hakem, N.L., Allen, P.G., Sylwester, E.R., 2001. Effect of EDTA on plutonium migration. J. Radioanal. Nucl. Chem. 250, 47–53. https://doi.org/10.1023/A:1013260029269.

Hummel, W., 2009. Ionic Strength Corrections and Estimation of SIT Ion Interaction Coefficients (PSI Technical Report). Paul Scherrer Institut, Villigen, Switzerland.

Hummel, W., Anderegg, G., Puigdomènech, I., Rao, L., Tochiyama, O., 2005. Chemical Thermodynamics of Compounds and Complexes of U, Np, Pu, Am, Tc, Se, Ni and Zr With Selected Organic Ligands, Chemical Thermodynamics. OECD Nuclear Energy Agency, Issy-les-Moulineaux, France.

IAEA, 2003. Scientific and Technical Basis for the Geologic Disposal of Radioactive Wastes (No. 413), Technical Reports Series. International Atomic Energy Agency, Vienna, Austria.

Kalmykov, S.N., Choppin, G.R., 2000. Mixed $Ca^{2+}/UO^{22+}/CO^{32}$ complex formation at different ionic strengths. Radiochim. Acta 88, 603–608. https://doi.org/10.1524/ract.2000.88.9-11.603.

Kinniburgh, D.G., Cooper, D.M., 2011. PhreePlot: Creating Graphical Output With PHREEQC. Centre for Ecology and Hydrology, Bangor, Gwynedd, UK.

Lee, J.-Y., Yun, J.-I., 2013. Formation of ternary $CaUO_2(CO_3)^{32}$ and $Ca_2UO_2(CO_3)_3(aq)$ complexes under neutral to weakly alkaline conditions. Dalton Trans. 42, 9862–9869. https://doi.org/10.1039/C3DT50863C.

Lemire, R.J., Garisto, F., 1989. The Solubility of U, Np, Pu, Th and Tc in a Geological Disposal Vault for Used Nuclear Fuel (No. AECL—10009). Atomic Energy of Canada Ltd.

Lucchini, J.F., Borkowski, M., Khaing, H., Richmann, M.K., Swanson, J.S., Simmons, K., Reed, D.T., 2013. WIPP Actinide-Relevant Brine Chemistry (No. LANL-CO ACRSP LCO-ACP-15).

McFadden, K.M., 1980. Organic Components of Nuclear Wastes and their Potential for Altering Radionuclide Distribution When Released to Soil (No. PNL-2563). Battelle Pacific Northwest Labs., Washington, DC.

Merciny, E., Gatez, J.M., Duyckaerts, G., 1978. Constantes de formation des complexes de stoechiometrie 1:1 et 1:2 ainsi que des complexes mixtes formes entre le plutonium (III) et divers acides amino-polyacetiques. Anal. Chim. Acta 100, 329–342. https://doi.org/10.1016/S0003-2670(01)93328-8.

Meyer, M., Burgat, R., Faure, S., Batifol, B., Hubinois, J.-C., Chollet, H., Guilard, R., 2007. Thermodynamic studies of actinide complexes. 1. A reappraisal of the solution equilibria between plutonium(IV) and ethylenediaminetetraacetic acid (EDTAH4) in nitric media. Comptes Rendus Chimie 10, 929–947. https://doi.org/10.1016/j.crci.2007.04.006.

Mikhailov, V.A., 1969. Investigation of the solubility of plutonium arylarsonates. Zh. Neorg. Khim. 14, 2133–2138.

Moskvin, A.I., Artyukhin, P.I., 1959. Determination of the composition and instability constants of Pu(III) ethylenediaminetetraacetate complexes by ion-exchange. Zh. Neorg. Khim. 4, 269–271.

Neck, V., Kim, J.I., 2001. Solubility and hydrolysis of tetravalent actinides. Radiochim. Acta 89, 1–16. https://doi.org/10.1524/ract.2001.89.1.001.

Neck, V., Altmaier, M., Rabung, T., Lützenkirchen, J., Fanghänel, T., 2009. Thermodynamics of trivalent actinides and neodymium in NaCl, $MgCl_2$, and $CaCl_2$ solutions: solubility, hydrolysis, and ternary Ca-M(III)-OH complexes. Pure Appl. Chem. 81, 1555–1568. https://doi.org/10.1351/PAC-CON-08-09-05.

Parkhurst, D.L., Appello, C.A.J., 1999. User's Guide to PHREEQC (Version 2) – A Computer Program for Speciation, Batch Reaction, One-dimensional Transport, and Inverse Geochemical Calculations (Water Resources Investigations Report No. 99–4259). USGS, Denver, Colorado, USA.

Parkhurst, D.L., Appello, C.A.J., 2013. Description of Input and Examples for PHREEQC Version 3—A Computer Program for Speciation, Batch-reaction, One-dimensional Transport, and Inverse Geochemical Calculations. U.S. Geological Survey Techniques and Methods. U.S. Department of the Interior, U.S. Geological Survey, Reston, Virginia, USA.

Pitzer, K.S., 1991. Ion Interaction Approach: Theory and Data Correlation in Activity Coefficients. Electrolyte Solutions. CRC Press, Boca Raton, FL, pp. 75–153.

Poczynajło, A., 1989. Potentiometric determination of Pu(III) complexes formed by citric acid, EDTA, DHTP and DTPP. J. Radioanal. Nucl. Chem. Artic. 134, 97–108. https://doi.org/10.1007/BF02047274.

Poczynajło, A., 1991. Extraction study of Pu(III)—EDTA chelates. J. Radioanal. Nucl. Chem. Artic. 148, 295–307. https://doi.org/10.1007/BF02060363.

Puigdomenech, I., 2020. Medusa/Spana.

Rai, D., Bolton, H., Moore, D.A., Hess, N.J., Choppin, G.R., 2001. Thermodynamic model for the solubility of PuO2(am) in the aqueous Na+-H+-OH–Cl–H_2O-ethylenediaminetetraacetate system. Radiochim. Acta 89, 67–74. https://doi.org/10.1524/ract.2001.89.2.067.

Rai, D., Moore, D.A., Rosso, K.M., Felmy, A.R., Bolton, H., 2008. Environmental mobility of Pu(IV) in the presence of ethylenediaminetetraacetic acid: myth or reality? J. Solut. Chem. 37, 957–986. https://doi.org/10.1007/s10953-008-9282-2.

Rai, D., Moore, D.A., Felmy, A.R., Rosso, K.M., Bolton, H., 2010. $PuPO_4$(cr, hyd.) solubility product and Pu^{3+} complexes with phosphate and ethylenediaminetetraacetic acid. J. Solut. Chem. 39, 778–807. https://doi.org/10.1007/s10953-010-9541-x.

Rand, M., Fuger, J., Grenthe, I., Neck, V., Rai, D., 2008. Chemical Thermodynamics of Thorium, Chemical Thermodynamics. OECD Nuclear Energy Agency, Issy-les-Moulineaux, France.

Ravel, B., Newville, M., 2005. ATHENA, ARTEMIS, HEPHAESTUS: data analysis for X-ray absorption spectroscopy using IFEFFIT. J. Synchrotron Radiat. 12, 537–541. https://doi.org/10.1107/S0909049505012719.

Reed, D.T., Wygmans, D.G., Aase, S.B., Banaszak, J.E., 1998. Reduction of Np(VI) and Pu(VI) by organic chelating agents. Radiochim. Acta 82, 109–114. https://doi.org/10.1524/ract.1998.82.special-issue.109.

Rojo, H., Gaona, X., Rabung, T., Polly, R., Garcia-Gutierrez, M., Missana, T., Altmaier, M., 2021. Complexation of Nd(III)/Cm(III) with gluconate in alkaline NaCl and $CaCl_2$ solutions: solubility, TRLFS and DFT studies. Appl. Geochem. 126, 104864.

Rothe, J., Butorin, S., Dardenne, K., Denecke, M.A., Kienzler, B., Löble, M., Metz, V., Seibert, A., Steppert, M., Vitova, T., Walther, C., Geckeis, H., 2012. The INE-beamline for actinide science at ANKA. Rev. Sci. Instrum. 83, 043105. https://doi.org/10.1063/1.3700813.

Rothe, J., Altmaier, M., Dagan, R., Dardenne, K., Fellhauer, D., Gaona, X., González-Robles Corrales, E., Herm, M., Kvashnina, K.O., Metz, V., Pidchenko, I., Schild, D., Vitova, T., Geckeis, H., 2019. Fifteen years of radionuclide research at the KIT synchrotron source in the context of the nuclear waste disposal safety case. Geosciences 9, 91. https://doi.org/10.3390/geosciences9020091.

Runde, W.H., 2000. The Chemical Interactions of Actinides in the Environment. Los Alamos Science, pp. 392–411.

Samuels, W.D., Camaioni, D.M., Babad, H., 1994. Initial Laboratory Studies into the Chemical and Radiological Aging of Organic Materials in Underground Storage Tanks at the Hanford Complex (No. PNL-SA--23331). Pacific Northwest Lab.

Schwarzenbach, G., Ackermann, H., 1947. Komplexone V. Die Äthylendiamintetraessigsäure. Helvetica Chimica Acta 30, 1798–1804. https://doi.org/10.1002/hlca.19470300649.

Stepanov, A.V., Makarova, T.P., 1965. Electromigration investigation of the complex formation of trivalent plutonium in solutions of ethylenediaminetetraacetic acid. Sov. Radiachem. 7, 663–668.

Tasi, A., Gaona, X., Fellhauer, D., Böttle, M., Rothe, J., Dardenne, K., Polly, R., Grivé, M., Colàs, E., Bruno, J., Källström, K., Altmaier, M., Geckeis, H., 2018a. Thermodynamic description of the plutonium – α-d-isosaccharinic acid system I: solubility, complexation and redox behavior. Appl. Geochem. 98, 247–264. https://doi.org/10.1016/j.apgeochem.2018.04.014.

Tasi, A., Gaona, X., Fellhauer, D., Böttle, M., Rothe, J., Dardenne, K., Polly, R., Grivé, M., Colàs, E., Bruno, J., Källstrom, K., Altmaier, M., Geckeis, H., 2018b. Thermodynamic description of the plutonium – α–d–isosaccharinic acid system ii: formation of quaternary Ca(II)–Pu(IV)–OH–ISA complexes. Appl. Geochem. 98, 351–366. https://doi.org/10.1016/j.apgeochem.2018.06.014.

Tasi, A., Gaona, X., Fellhauer, D., Böttle, M., Rothe, J., Dardenne, K., Schild, D., Grivé, M., Colàs, E., Bruno, J., Källström, K., Altmaier, M., Geckeis, H., 2018c. Redox behavior and solubility of plutonium under alkaline, reducing conditions. Radiochim. Acta 106, 259–279. https://doi.org/10.1515/ract-2017-2870.

Thakur, P., Pathak, P.N., Choppin, G.R., 2009. Complexation thermodynamics and the formation of the binary and the ternary complexes of tetravalent plutonium with carboxylate and aminocarboxylate ligands in aqueous solution of high ionic strength. Inorg. Chim. Acta 362, 179–184. https://doi.org/10.1016/j.ica.2008.03.127.

Tits, J., Wieland, E., Bradbury, M.H., 2005. The effect of isosaccharinic acid and gluconic acid on the retention of Eu(III), Am(III) and Th(IV) by calcite. Appl. Geochem. 20, 2082–2096. https://doi.org/10.1016/j.apgeochem.2005.07.004.

US NRC, 2020. Full-text Glossary.

Vercammen, K., Glaus, M.A., Loon, L.R.V., 2001. Complexation of Th(IV) and Eu(III) by α-isosaccharinic acid under alkaline conditions. Radiochim. Acta 89, 393–402. https://doi.org/10.1524/ract.2001.89.6.393.

Wieland, E., Van Loon, L.R., 2003. Cementitious Near-Field Sorption Data Base for Performance Assessment of an ILW Repository in Opalinus Clay (No. PSI–03-06). Paul Scherrer Institut.

Wyckoff, R.W.G., 1963. Crystal Structures. 2nd ed. Interscience Publishers, New York, New York.

Karlsruher Institut für Technologie

OPEN ACCESS

Repository KITopen

Dies ist ein Postprint/begutachtetes Manuskript.

Empfohlene Zitierung:

DiBlasi, N. A.; Tasi, A. G.; Gaona, X.; Fellhauer, D.; Dardenne, K.; Rothe, J.; Reed, D. T.; Hixon, A. E.; Altmaier, M.
Impact of Ca(II) on the aqueous speciation, redox behavior, and environmental mobility of Pu(IV) in the presence of EDTA
2021. The science of the total environment, 783
doi: 10.554/IR/1000131553

Zitierung der Originalveröffentlichung:

DiBlasi, N. A.; Tasi, A. G.; Gaona, X.; Fellhauer, D.; Dardenne, K.; Rothe, J.; Reed, D. T.; Hixon, A. E.; Altmaier, M.
Impact of Ca(II) on the aqueous speciation, redox behavior, and environmental mobility of Pu(IV) in the presence of EDTA
2021. The science of the total environment, 783, 146993.
doi:10.1016/j.scitotenv.2021.146993

Lizenzinformationen: CC BY-NC-ND 4.0